GEOLOGICA CARPATHICA, FEBRUARY 2009, 60, 1, 15–33 doi: 10.2478/v10096-009-0001-8

The emplacement mode of Upper Cretaceous plutons from the southwestern part of the Sredna Gora Zone (Bulgaria): structural and AMS study

NEVEN GEORGIEV[1*], BERNARD HENRY[2], NELI JORDANOVA[3], NIKOLAUS FROITZHEIM[4], DIANA JORDANOVA[3], ZIVKO IVANOV[1] and DIMO DIMOV[1]

[1]Department of Geology and Paleontology, Sofia University "St. Kliment Ohridski" 15 Tzar Osvoboditel bd., 1000 Sofia, Bulgaria; neven@gea.uni-sofia.bg
[2]Paléomagnétisme, IPGP and CNRS, 4 av. de Neptune, 94107 Saint-Maur cedex, France
[3]Geophysical Institute, Bulgarian Academy of Sciences, Acad. G. Bonchev str., block 3, 1113 Sofia, Bulgaria
[4]Steinmann-Institut, Universität Bonn, Nußallee 8, D-53115 Bonn, Germany

(Manuscript received February 21, 2008; accepted in revised form June 12, 2008)

Abstract: Several plutons located in the southwestern part of the Sredna Gora Zone — Bulgaria are examples of the Apuseni-Banat-Timok-Sredna Gora type of granites emplaced during Late Cretaceous (86–75 Ma) times. The studied intrusive bodies are spatially related to and deformed by the dextral Iskar-Yavoritsa shear zone. The deformation along the shear zone ceased at the time of emplacement of the undeformed Upper Cretaceous Gutsal pluton, which has intruded the Iskar-Yavoritsa mylonites. A clear transition from magmatic foliation to high-, moderate- and low-temperature superimposed foliation and lineation in the vicinity of the Iskar-Yavoritsa and related shear zones gives evidence for simultaneous tectonics and plutonism. Away from the shear zones, the granitoids appear macroscopically isotropic and were investigated using measurements of anisotropy of magnetic susceptibility at 113 stations. The studied samples show magnetic lineation and foliation, in agreement with the magmatic structures observed at a few sites. Typical features of the internal structure of the plutons are several sheet-like mafic bodies accompanied by swarms of mafic microgranular enclaves. Field observations indicate spatial relationships between mafic bodies and shear zones as well as mingling processes in the magma chamber which suggest simultaneous shearing and magma emplacement. Structural investigations as well as anisotropy of magnetic susceptibility (AMS) data attest to the controlling role of the NW-SE trending Iskar-Yavoritsa shear zone and to the syntectonic emplacement of the plutons with deformation in both igneous rocks and their hosts. The tectonic situation may be explained by partitioning of oblique plate convergence into plate-boundary-normal thrusting in the Rhodopes and plate-boundary-parallel transcurrent shearing in the hinterland (Sredna Gora).

Key words: Late Cretaceous, Sredna Gora — Bulgaria, tectonics, magma emplacement, strike-slip setting, AMS.

Introduction

The role of shear zones in the generation, ascent and emplacement of magma through the crust is a long-standing matter of debate (Castro 1987; Hutton 1988, 1997; Paterson & Fowler 1993; Acef et al. 2003; Rosenberg 2004). Numerous examples of granite emplacement along strike-slip fault systems in transpressional or transtensional tectonic settings (Tikoff & Teyssier 1992; Paterson & Fowler 1993; Roman-Berdiel et al. 1997; Steenken et al. 2000; Henry et al. 2004) suggest different possibilities to solve the "space problem". Visible structures of the granitoids formed in the magmatic stage and superimposed solid-state foliations and lineations provide valuable information on magma emplacement kinematics and can help us to better understand the connection between tectonics and magmatism (Saint Blanquat & Tikoff 1997; Steenken et al. 2000). The latter is not a simple task, especially when the studied intrusives are nearly isotropic and widely used structural methods are not applicable. In such cases the measurement of Anisotropy of Magnetic Susceptibility (AMS) is a standard procedure (Tarling & Hrouda 1993). Determination of magnetic fabric is a quick and easy semi-quantitative method to provide information on the bulk fabric of the plutons (Henry 1980; Bouchez 1997; Saint Blanquat & Tikoff 1997). The results are often used to support structural data in constraining the syn- or post-tectonic emplacement of intrusions (Henry 1980; Bouchez 1997; Henry et al. 2004).

On the other hand, some studies (Ferre et al. 1997) demonstrate that crustal-scale shear zones play a role of feeder channels and can provide space for chamber formation at different depths. These relationships can explain the frequent coexistence of magmas contrasting in composition (felsic and mafic) at the same crustal level (Michael 1991; Wiebe & Collins 1998). Interaction between contrasting magmas (mixing versus mingling processes) depends on parameters like volume, time, compositions, temperature, viscosity, etc. (Barbarin & Didier 1992).

The Upper Cretaceous intrusive bodies located in the southwestern part of the Sredna Gora Zone, Bulgaria, crop out in close relationship with the regional dextral strike-slip Iskar-Yavoritsa shear zone (IYSZ). The aim of this study is to investigate the space- and time connection between plutons and shear zone using structural and AMS data, and to provide a model for emplacement of these granites.

Geological setting

The Sredna Gora Zone in Bulgaria is a part of a complex, elongated Late Cretaceous–Tertiary magmatic arc that can be traced from the Apuseni Mountains in Romania to Iran (Bergougnan & Fourquin 1980; Sandulescu 1984; Mitchell 1996; Jankovic 1977, 1997; Berza et al. 1998; Stampfli & Mosar 1999; Neubauer 2002). This zone is regarded as a volcanic island arc (Boccaletti et al. 1974, 1978), back-arc basin (Hsu et al. 1977) or intra-arc basin with submarine volcanism (Nachev 1978). According to Dabovski (1980) the Sredna Gora Zone represents an intracontinental rift, which originated in connection with the Vardar subduction. Intrusive and volcanic rocks, the products of Upper Cretaceous magmatic activity, are widespread in the Sredna Gora Zone.

According to Ivanov (1989) the studied plutons (Fig. 1) were emplaced at the boundary between two different metamorphic terranes (Balkanide terrane to the North and Rhodope terrane to the South), separated by the dextral strike-slip IYSZ. The northern terrane (Balkanide metamorphic complex; Ivanov 1988, 1989) is built up of Variscan high-grade metamorphic rocks metamorphosed at 320–340 Ma and of 315 to 289 Ma old granitoid bodies (Amov et al. 1982; Velichkova et al. 2001, 2004; Carrigan et al. 2005, 2006). To the south of the IYSZ the Rhodope terrane is represented by the variegated unit, including ortho- and para-metamorphic rocks (Ivanov et al. 2000). The age of metamorphism in this part of the Rhodope terrane is still unknown. The variegated unit is equivalent to the Asenitsa Unit further east in the Central Rhodopes. U-Pb zircon data give evidence for Jurassic (~150 Ma) magmatic protoliths of Asenica gneisses to the SE of the studied area (von Quadt et al. 2006). In the Late Cretaceous, the rocks of the Rhodope terrane in our study area must already have been exhumed to a level between the middle and upper crust because they were intruded by the granites (Georgiev & Lazarova 2003).

In the southwestern part of the Sredna Gora Zone (Fig. 1), several Upper Cretaceous plutonic bodies (Plana, Gutsal and Elshitsa-Boshulia) and the "Variscan" Varshilo intrusion (Dimitrov 1933; Boyadjiev 1979 and references therein; Dabovski 1980, 1988 and references therein; Belmustakova 1984) were distinguished. These plutons form a WNW-ESE-trending complex belt on both sides of the IYSZ. Previous interpretations regard the Upper Cretaceous magmatic bodies as a result of multiphase or two-phase intrusions with normal partial differentiation of basaltic magma. Considering emplacement mechanisms, Dabovski (1988) suggested that the plutons are "fissure intrusions" formed in a rift setting.

The plutons comprise two different groups of rocks: felsic (granites and granodiorites) and mafic to intermediate (gabbros, quartz-monzogabbros, quartz-monzodiorites and quartz-diorites). The mafic varieties were supposed to be older, numerous mafic enclaves in the granites and granodiorites being regarded as xenoliths from the country rocks-

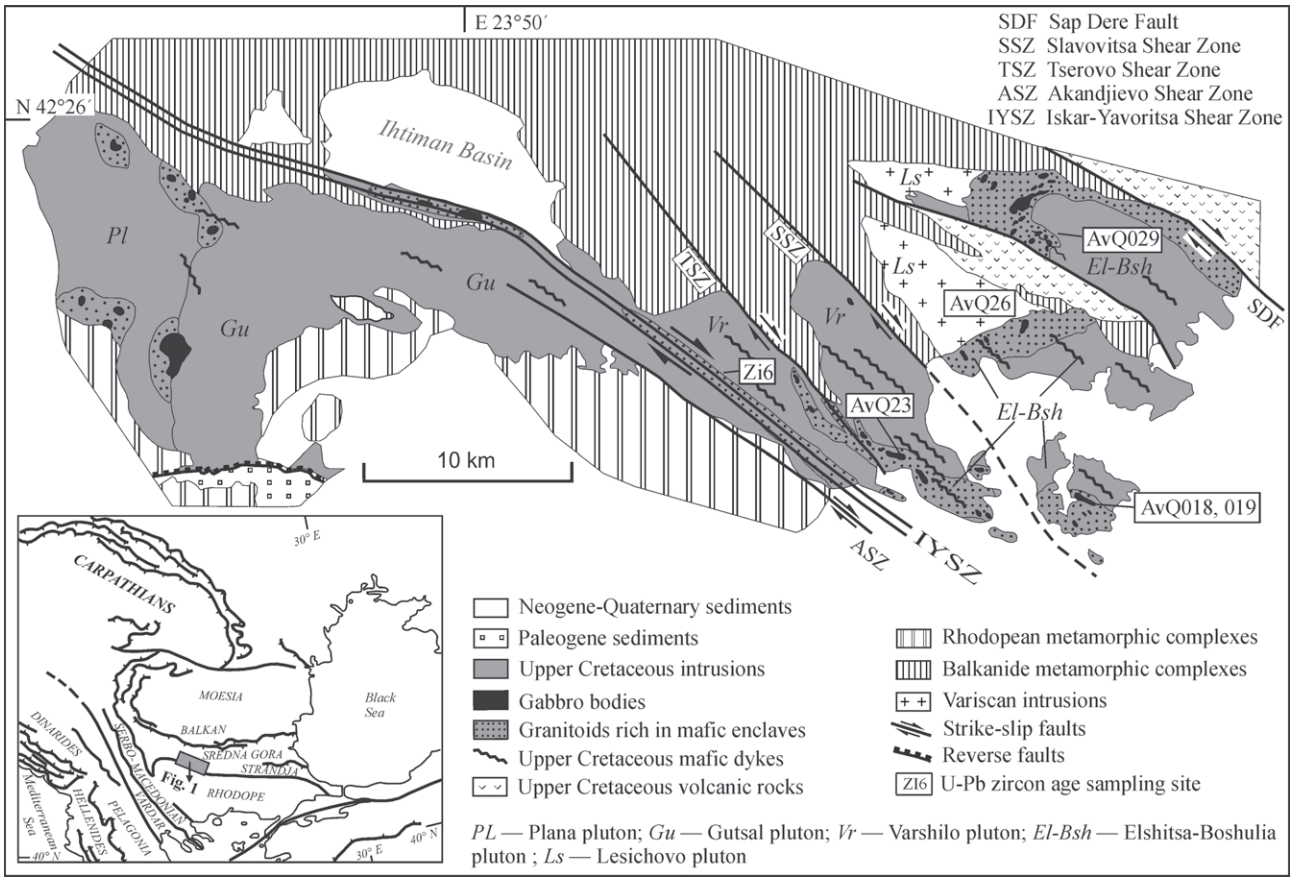

Fig. 1. Simplified geological map of the southwestern parts of the Sredna Gora Zone.

Table 1: U-Pb zircon ages for intrusive rocks from the southern parts of Central Sredna Gora.

Sample	Pluton	Locality	Rock type	Age and 2σ error (Ma)	Reference
AvQ029	Elshitsa-Boshulia	2 km NW of Elshitsa village	granite	86.62 ± 0.11	Peytcheva et al. (2003)
AvQ019	Elshitsa-Boshulia	Velichkovo quarry	granodiorite	84.6 ± 0.3	von Quadt et al. (2005)
AvQ018	Elshitsa-Boshulia	Velichkovo quarry	hybrid gabbro	82.16 ± 0.10	von Quadt et al. (2005)
AvQ023	Elshitsa-Boshulia	Vetrensko Gradishte	hybrid gabbro	84.87 ± 0.13	von Quadt et al. (2005)
ZI6	Varshilo	2.5 km W of Dolno Varshilo village	granite	82.25 ± 0.22	von Quadt et al. (2005)
AvQ026	Lesichovo	1 km N of Lesichovo village	granite	316.5 ± 3.5	Peytcheva & von Quadt (2003)

gabbros and basic volcanics. The major element compositions of the granitoids are typical for calc-alkaline and island-arc magmatic products. The compositions of mafic rocks correspond to tholeiitic and to calc-alkaline varieties.

Recently obtained U-Pb data (Peytcheva et al. 2001; Peytcheva & von Quadt 2003) indicate small differences between the ages of granites — 82 Ma, granodiorites — 86–84 Ma, and gabbros — 82–84 Ma (Table 1). The dating of the Varshilo pluton, previously assumed to be Variscan, yielded a Late Cretaceous (82 Ma) age. Unpublished U-Pb zircon data (Georgiev, von Quadt & Peytcheva) from the Gutsal granodiorite yielded a ~75 Ma age of crystallization. This younger age is supported by the field relationships: the Varshilo granites are sheared in the vicinity of IYSZ whereas sills of Gutsal granodiorite are undeformed and have intruded the IYSZ mylonitic foliation.

Thermo-barometrical data (Georgiev & Lazarova 2003) show that the emplacement of granodioritic melts took place under pressures between 470 MPa (corresponding to a depth of ca. 13 km) and 320 MPa (ca. 9 km).

Structures of the plutons

Magmatic and submagmatic structures

The plutonic bodies mostly appear macroscopically isotropic. Nevertheless, magmatic foliation is often visible close to the plutonic contacts or forms bands parallel and related to the IYSZ and its associated shear zones. Far from mylonitic domains, magmatic foliation is less pronounced and oblique to the shear zones. Near undeformed plutonic contacts, magmatic foliation is parallel both to the contacts and to the host rock's schistosity. The magmatic foliation is defined by the preferred orientation of biotite, feldspar and hornblende crystals (Fig. 2a,d) as well as mafic microgranular enclaves (Fig. 2b). Magmatic layering is observed in some gabbro bodies (Fig. 2c), defined by layers of different mineral proportion and/or different grain size of the rock-forming minerals. The magmatic foliation predominantly trends 100–140° and dips steeply (45–90°) towards the NE or the SW (Fig. 3). The magmatic lineation data are too scarce to be representative and informative. The magmatic lineation is defined mostly by alignment of hornblende, biotite and quartz-feldspar aggregates (Fig. 2a) and in some places by mafic enclaves.

Microfractures in feldspar phenocrysts are filled with residual melt represented by magmatic quartz (Fig. 4a and b) which is typical for a submagmatic stage of deformation (Bouchez et al. 1992). Thin section investigations of samples with visible magmatic foliation show parallel alignment of elongated feldspar crystals (Fig. 4c). The initial stages of subgrain formation observed in potassium feldspars, together with the lack of any other deformation in the samples with visible magmatic foliation, suggest transitional submagmatic to high-temperature solid-state deformation (Fig. 4d).

Shear zones and solid-state deformation

In a regional view, important structures in the studied area are the IYSZ and related shear zones (Fig. 1). The IYSZ is an 80–90 km long and 0.4–1.0 km wide shear zone with general strike of 110–130° and steep dips (60–80°) toward the NE to SW. In the vicinity of the IYSZ, several satellite shear zones of similar orientations, kinematics and deformation features were recognized (Fig. 1): the Akandjievo shear zone (ASZ), Slavovitsa shear zone (SSZ), Tserovo shear zone (TSZ) and Sapdere fault (SDF). The deformation degree increases in narrow (15 to 40 m thick) mylonitic bands within the shear zones where the studied plutons as well as their host rocks are transformed into mylonites. The deformation style grades from ductile (high-temperature) in outer parts of the shear zones to brittle-ductile within the inner parts. Mica bands and elongated quartz-feldspar aggregates define the foliation. Elongated biotite flakes and quartz grains trace the mineral lineation on the foliation planes. Striations are rarely found on the foliation planes in domains with brittle-ductile overprint. The mineral lineation plunges 5 to 50° to the NW or is subhorizontal (Fig. 3).

High-temperature solid sate deformation

In the field, domains with a high-temperature solid-state deformation are located at the transition between intensively deformed parts of the shear zones and areas with a magmatic foliation. Most of the outcrops show clear relationship between roughly NW-SE-trending vertical foliation and steeply dipping or vertical c'-shear bands (Fig. 5a). In the outcrops with many mafic microgranular enclaves, the s–c' pattern has produced "enclave fish" which are reliable criteria indicating dextral kinematics. Quartz with mosaics of square subgrains and chessboard patterns (Fig. 5b) indicates high-temperature solid-state deformation (>ca. 650°; Kruhl 1996; Stipp et al. 2002; Passchier & Trouw 2005). Feldspar grains with core-and-mantle structure (Fig. 5d) may represent a transitional stage (450° to 500 °C; Passchier & Trouw 2005) between this high-temperature deformation and the colder deformation stages described below.

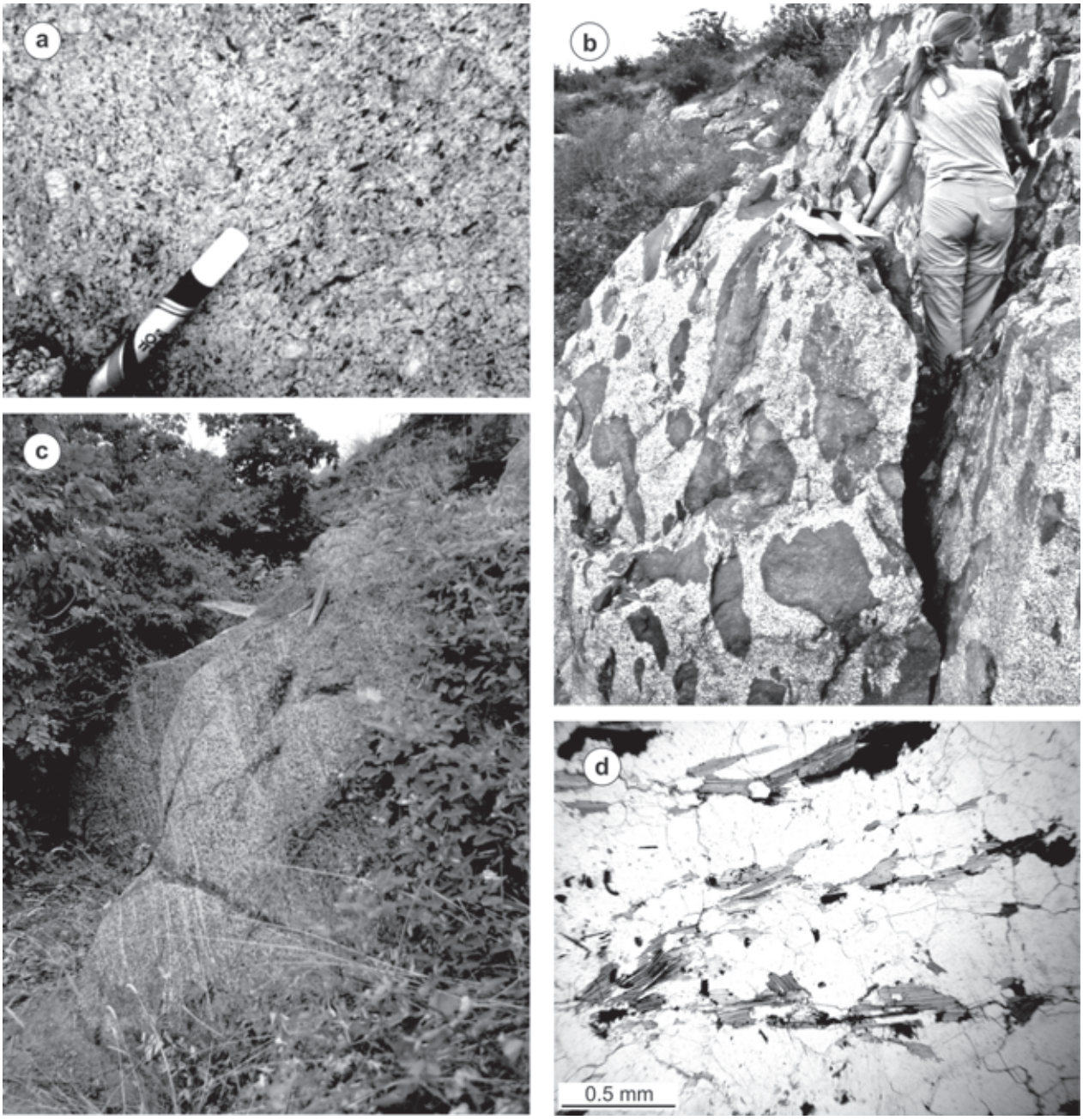

Fig. 2. Field and micrographic examples of primary magmatic structures for the studied igneous rocks. **a** — Magmatic foliations defined by preferred orientation of feldspar and hornblende crystals in granodiorite. **b** — Magmatic foliation defined by stretched mafic microgranular enclaves within granodiorites host. **c** — The magmatic layering of gabbroic sheets is commonly observed. The separate layers are defined by differences in mineral composition or by differences in size of rock-forming minerals. **d** — Photomicrograph of a granite with magmatic foliation defined by ordered biotite and rare feldspar crystals.

Moderate- to low-temperature solid-state deformation

Moderate- to low-temperature structures are typical for high-strain bands within the inner parts of the IYSZ system where gneissification and s–c granitoid mylonites are observed (Fig. 6a). In some places the granitoids were transformed into quartz-chlorite ultramylonites (Fig. 6b). Moderate- to low-temperature deformation has produced microstructures at decreasing temperatures during shearing: high-angle undulose extinction and subgrains are ubiquitous in quartz; biotite is partly or totally replaced by chlorite; feldspar porphyroclasts contain deformational myrmekites (Fig. 6c). The matrix of the mylonites was ductile but the feldspars have responded to deformation as brittle rigid objects (Fig. 6d) and formed "book shelves" and "v"-pull apart microstructures (Hippertt 1993). Criteria within intensively deformed parts of the shear zones consistently show dextral shear sense (Fig. 6a,d; Fig. 7).

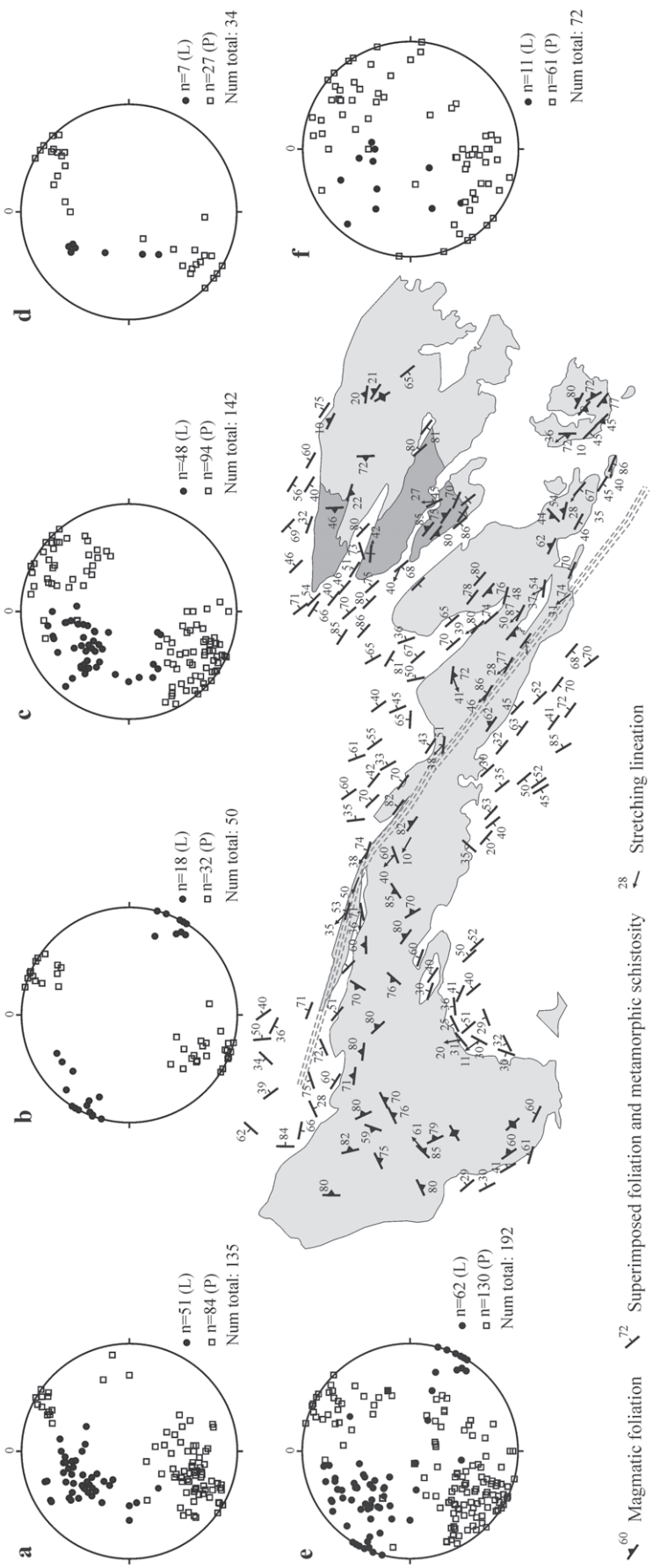

Fig. 3. Position of the observed magmatic and superimposed structures for plutonic bodies and metamorphic host rocks. Stereographic projection on lower hemisphere of superimposed foliations and lineations along: **a** — Iskar-Yavoritsa shear zone; **b** — Akandjievo shear zone; **c** — Slavovitsa shear zone; **d** — Tserovo shear zone; **e** — Foliation and stretching lineation of metamorphic host; **f** — Magmatic fabrics of granitoids.

Annealing process

In the vicinity of the Gutsal granite intrusion, quartz- and mica-rich mylonites of the IYSZ show evidence for post-kinematic annealing. In outcrop, these rocks appear like low-temperature mylonites and phyllonites. The microscopic observations show that these high-strain rocks were overprinted by relatively high-temperature static recrystallization (Fig. 5c,e,f). This is shown by polygonal quartz grains and foam structure in foliation-parallel quartz domains.

Magma mingling processes

Porphyritic granodiorites, granites, and gabbros are the major types of studied intrusive rocks. The field relationships are critical for interpreting the coexistence of felsic and mafic rocks within the plutons. Mafic rocks (gabbros, gabbro-diorites and diorites) build up several sheet-like or lensoid bodies (Fig. 1), ranging in size from 100–200 m^2 to 1.5–2 km^2 and in thickness from 30 to 100 m. These mafic bodies usually crop out inside granodioritic "matrix". Coarse-grained gabbros and/or gabbro-diorites compose the inner parts of the sheets (Fig. 8a). The bottom contacts of gabbroic sheets against granodiorites are chilled, sharp and often relatively straight (Fig. 8b). Load-cast (Fig. 8c,d) and flame structures (Fig. 8e) have been observed at these contacts. Such types of relations indicate interaction of nearly liquid felsic and mafic melts (see Wiebe & Collins 1998). Granites or granodiorites rich in mafic microgranular enclaves (Figs. 1, 8f) have a close spatial relation with the mafic bodies. As a rule, such levels are situated above and also to the sides of the mafic sheets. On the regional scale, the mafic sheets and the enclave-bearing rocks form almost continuous bands spatially related to the IYSZ and the associated shear zones (Fig. 1).

AMS study

In macroscopically isotropic rocks, AMS study is often the most efficient

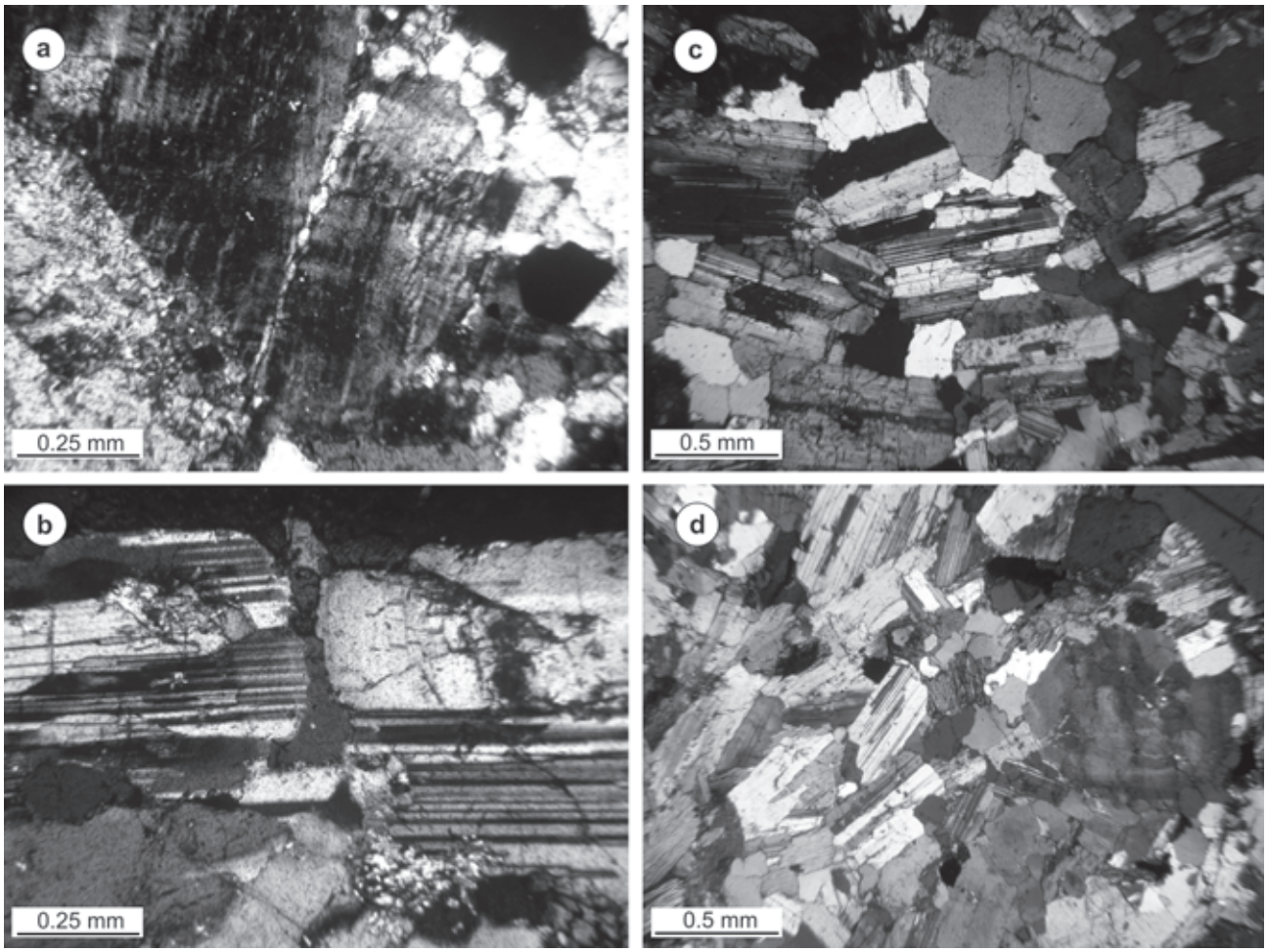

Fig. 4. Crossed-polar micrographic examples of primary magmatic structures and transition to submagmatic strain stage. Magmatic foliations defined by preferred orientation of feldspar crystals. **a** and **b** — Micro-fractures in feldspar phenocrysts filled with residual melt presented by magmatic quartz. **c** — Pronounced magmatic foliation is shown by a linear arrangement of tabular plagioclase crystals. **d** — Zoned K-feldspar showing an initial formation of sub-grains.

way for structural analysis. The AMS in low field is described by a symmetrical second-rank tensor. It is represented by a triaxial ellipsoid with principal directions and magnitudes Kmax, Kint, and Kmin. Fabric pointed out by AMS can reflect flow for magmatic rocks, deposition context for sediments or finite strain in deformed rocks (Borradaile & Henry 1997). The orientation of the susceptibility ellipsoid for low bulk susceptibilities ($K < 0.5 \times 10^{-3}$ SI) is directly related to the preferred crystallographic orientation of paramagnetic minerals, while in rocks possessing high ferromagnetic mineral content ($K > 10^{-3}$ SI), AMS ellipsoid is mainly determined by the shape and/or distribution of strongly magnetic minerals like magnetite and titanomagnetite.

Sampling and methods

Cores, oriented using magnetic and sun compasses, have been drilled with a portable gasoline drilling machine. Five to twelve samples per site were gathered from 113 sampling locations. The effect of possible local non-homogeneity of the granites was minimized by sampling in an area of several square meters at each outcrop. Sampling sites are evenly distributed in the study area, with the major exception of the westernmost parts (Plana pluton), where outcrop conditions allowed only a N-S profile. Several dykes, vein bodies and basic sheets genetically associated with the main magmatism were sampled as well.

AMS was measured with Kappabridge KLY-2 (Agico, Brno). Statistical analyses of the data were carried out using tensorial (Hext 1963; Jelinek 1978) and bivariate (Henry & Le Goff 1995) approaches. The magnetic zone axis was determined with its confidence zone (Henry 1997).

Identification of magnetic mineralogy was done by the Curie temperature indicated on the thermal behaviour of magnetic susceptibility K(T°C) in low field in the temperature range from room temperature up to 700 °C. This K(T°C) analysis was carried out with a CS-23 furnace attachment to the Kappabridge. Low-temperature susceptibility behaviour, down to the liquid nitrogen temperature (77 K) for selected samples, was used as an additional tool for mineral identification. Effective domain state of ferromagnetic carriers was

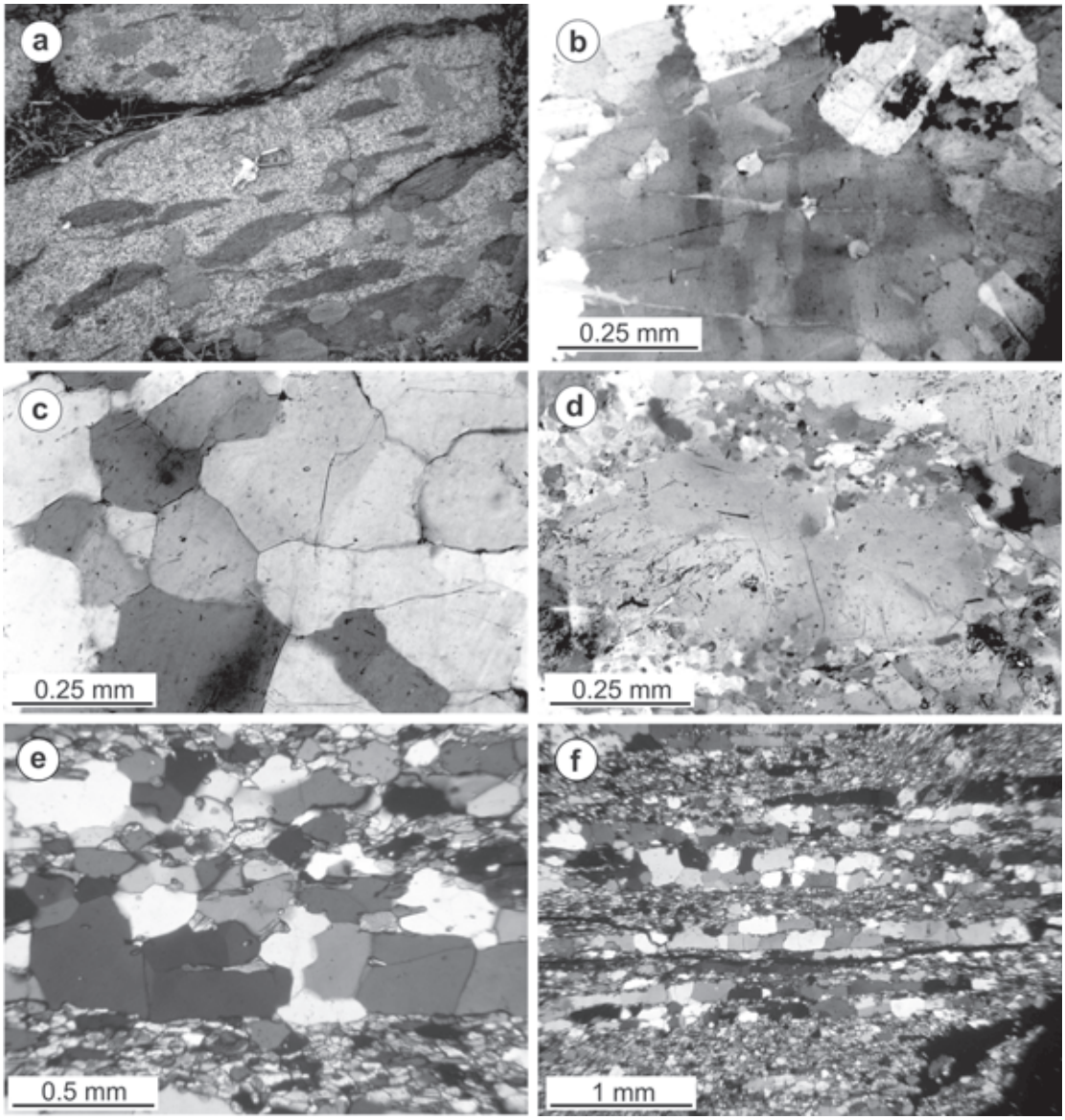

Fig. 5. Field photograph and crossed-polar micrographs of the high-temperature character of deformation within granitoids from the peripheral parts of the shear zones. **a** — Steeply dipping or vertical c'-shear bands 10 to 20 cm in size from the high-temperature deformational stage, indicating dextral shearing. **b** — High-temperature solid state overprint with chessboard pattern in quartz. **c** — High-temperature static overprint with polygonal quartz grains and foam structure formation. **d** — Core-mantle structure in K-feldspar indicating moderate temperature (~450 °C) solid state deformation. **e** and **f** — Annealed mylonitic granite from the central parts of IYSZ. The quartz layers were originally formed by deformation under decreasing temperatures. Polygonization of quartz grain boundaries is interpreted as resulting from a later temperature increase during intrusion of the Gutsal granodiorite.

deduced from the hysteresis curves, measured for bulk samples, using translation inductometer within an electromagnet capable of reaching 1.6 Tesla.

Magnetic properties of the studied rocks

Bulk susceptibility values

The measured magnetic susceptibility values vary in a wide range (from 37×10^6 up to 0.1 SI units). Lesichovo leucogranites and Elshitsa granodiorites are characterized by the lowest susceptibility values, probably mainly determined by the phyllosilicate content. The other intrusions, with significantly higher susceptibilities, show wider distributions, which is a typical characteristic of strongly magnetic granitoids. Values higher than 5×10^3 SI suggest that the ferromagnetic fraction plays the major role in determination of the shape and orientation of the magnetic susceptibility ellipsoid for most of the sites.

Magnetic mineralogy

Representative examples of the common K(T°C) behaviour are given in Figure 9. Most of the sites show an almost revers-

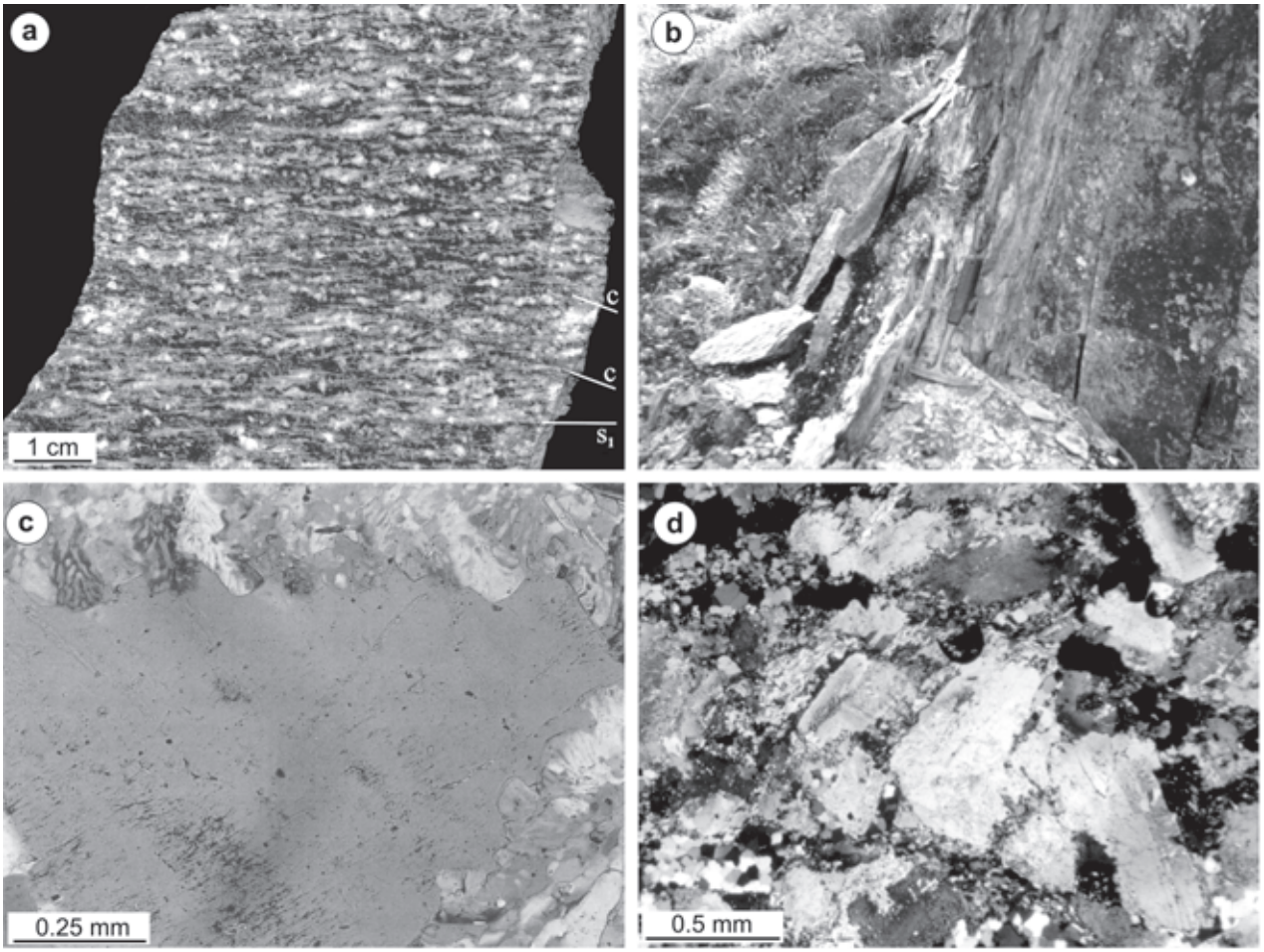

Fig. 6. Field photographs and crossed-polar micrographs of moderate to low-temperature character of deformation from the inner parts of IYSZ and related shear zones. **a** — s–c fabric in granodiorite polished hand specimen from the inner parts of IYSZ. **b** — Quartz-chlorite ultramylonites from the inner parts of IYSZ. **c** — K-feldspar porphyroclasts with deformational myrmekites. **d** — "Book shelves" and "v"-pull-apart microstructures indicating brittle behaviour of feldspars in contrast to ductile behaviour of the matrix.

ible K(T°C) heating-cooling cycle with a main Curie temperature (Tc) of 580 °C, indicating the presence of magnetite (see Dunlop & Özdemir 1997). Reversible peculiarity on some of the curves at 120–150 °C well expressed for some samples (see Fig. 9b — sample CF01 with the enlarged scale) is probably due to hemo-ilmenites, the end product of high-temperature exsolution. Another group of samples from the enclave-bearing level of Elshitsa and Boshulia plutons shows the presence of a significant drop in the signal at 350 °C followed by the well-expressed magnetite Tc (580 °C) as shown in Fig. 9a (sample X04). Correct interpretation of the nature (real Tc or transformation temperature) and source of this medium-temperature feature is not straightforward because of the existence of several minerals having Tc or transforming in this temperature range. Partial K(T°C) heating curves indicate reversible behaviour before the drop at 300 °C, but irreversible transformation after heating at 350 °C in air and cooling back to room temperature. Such behaviour may indicate progressive transformation of pyrrhotite (Bleil & Petersen 1982) in an oxidizing environment (Dekkers 1990). Most probably these Fe-sulphides are products of the late hydrothermal mineralization found in the area (Boyadjiev 1979 and references therein). Low temperature demagnetization down to –180 °C reveals clearly the dominant role of magnetite, identified by the presence of Verwey transition at about –160 °C (Fig. 10).

Hysteresis parameters

Hysteresis measurements carried out for original, non-separated material reveal mostly multidomain (MD) magnetite shapes of the loops and values of the hysteresis parameters (Hc, Hcr, Js, Jrs) (Table 2 and Fig. 11). The interpretation of the ratios Jrs/Js and Hcr/Hc in terms of magnetic domain state is favoured by the results from K(T°C) experiments as far as the latter show the major magnetite role and no indications about the presence of high coercivity phases, which would prevent the direct interpretation of Day diagrams (Day et al. 1977). Data points follow a single trend line (Fig. 11) through MD–PSD regions, suggesting mixing of different relative proportions of MD and SD grains (see the theoretical model of Dunlop 2002). The samples from the Elshitsa pluton (Fig. 11) show the highest stability, prob-

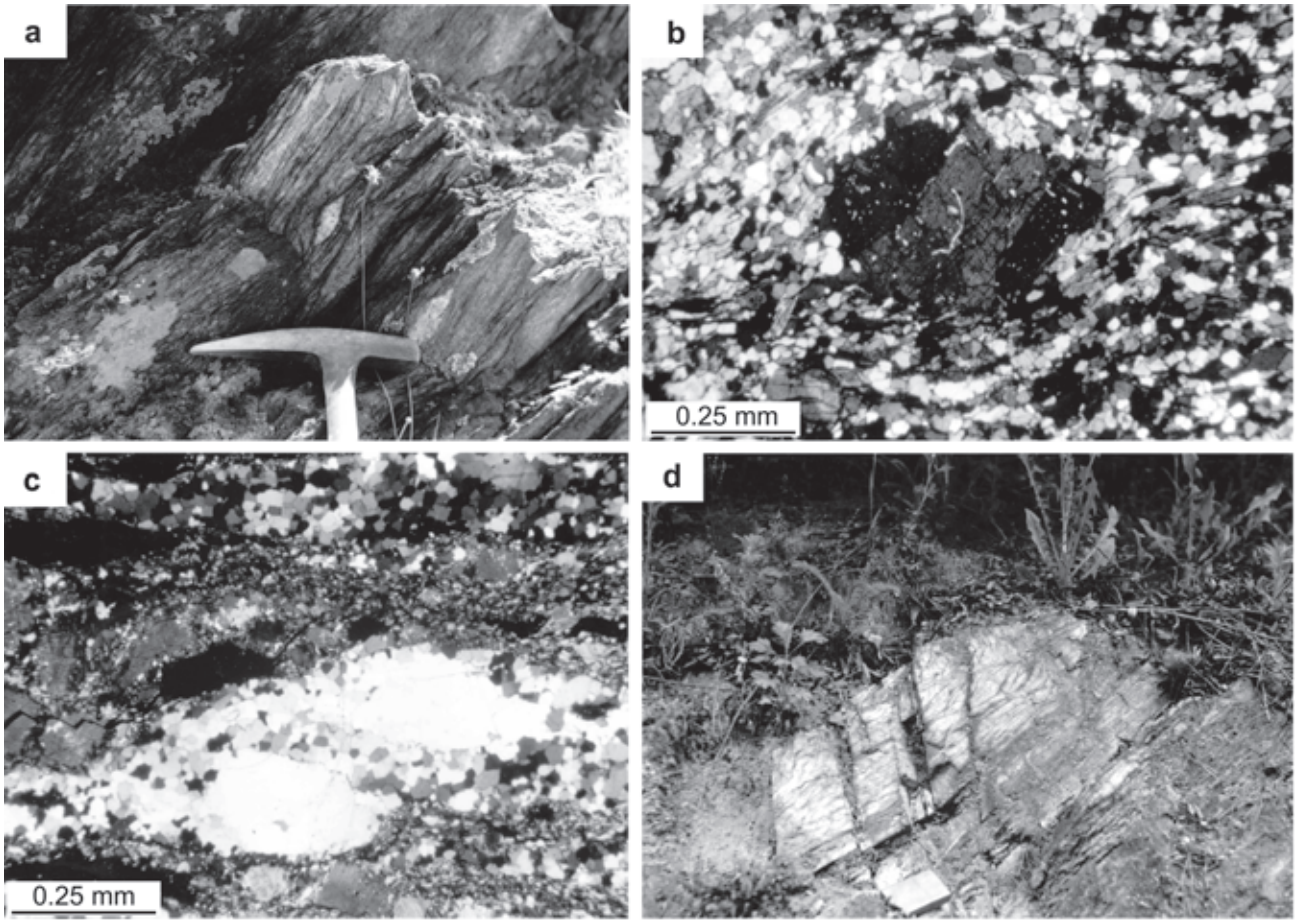

Fig. 7. a–c — Crossed-polar photomicrographs of δ-type feldspar porphyroclasts; a — shear bands. **d** — Foliation "fishes". All the criteria indicate dextral kinematics of the shear zones.

ably influenced by the possible presence of pyrrhotite. Samples from the Lesichovo leucocratic granites present a paramagnetic behaviour. As a whole, granodiorites from the Elshitsa and Lesichovo intrusions show relatively higher coercivities (Table 2).

Since most magnetite generally crystallizes at temperatures lower than the largest part of the melt, it will mimic the crystallographic preferred orientation of the initially formed minerals reflecting the last stages of magma crystallization (Hrouda et al. 1971). Thus, the MD magnetite grains have shapes and orientations determining a magnetic susceptibility ellipsoid consistent in orientation with the crystallographic ordering of the main rock-forming minerals. The elements of the measured magnetic fabric (magnetic foliation and lineation) could then reliably indicate the magmatic fabric in the studied plutons.

Magnetic fabric of the main intrusive bodies

Directional data

Magmatic and high-temperature (HT) visible foliation has been observed only at 31 of the sampled sites, magmatic visible lineation only at 13 sites and post-magmatic moderate- to low temperature (M-LT) foliation only in 4 other sites. These are traced by specific orientations of K-feldspars, biotite crystals or enclaves.

The distribution of the different principal susceptibility axes on a scale of sampling site shows quite good grouping in all but 6 % of the sites, situated away from the shear zone and showing scattered patterns. Girdle distributions of Kmax or Kmin directions, not caused by measurement uncertainty, are, however, observed in the sites with high oblateness/prolateness due to the similar values of the principal susceptibility Kmax/Kmin with that of Kint. The directional AMS data representing the poles to magnetic foliation (Kmin axes) and magnetic lineation (Kmax axes) agree with those of the field magmatic structures close to the IYSZ zone. The orientations are very coherent and parallel to the shear zone (Fig. 12). On the contrary, low temperature foliations appear to be different from the magnetic foliation. The magnetic fabric is therefore related to the conditions during the magma emplacement. Farther from the IYSZ, orientation of the different principal susceptibilities is more variable, probably corresponding to conditions of magma emplacement less constrained by shearing. The top-facies of the plutons represented by Elshitsa-Boshulia granodiorites, showing rather different directions of magnetic lineation, may also reflect

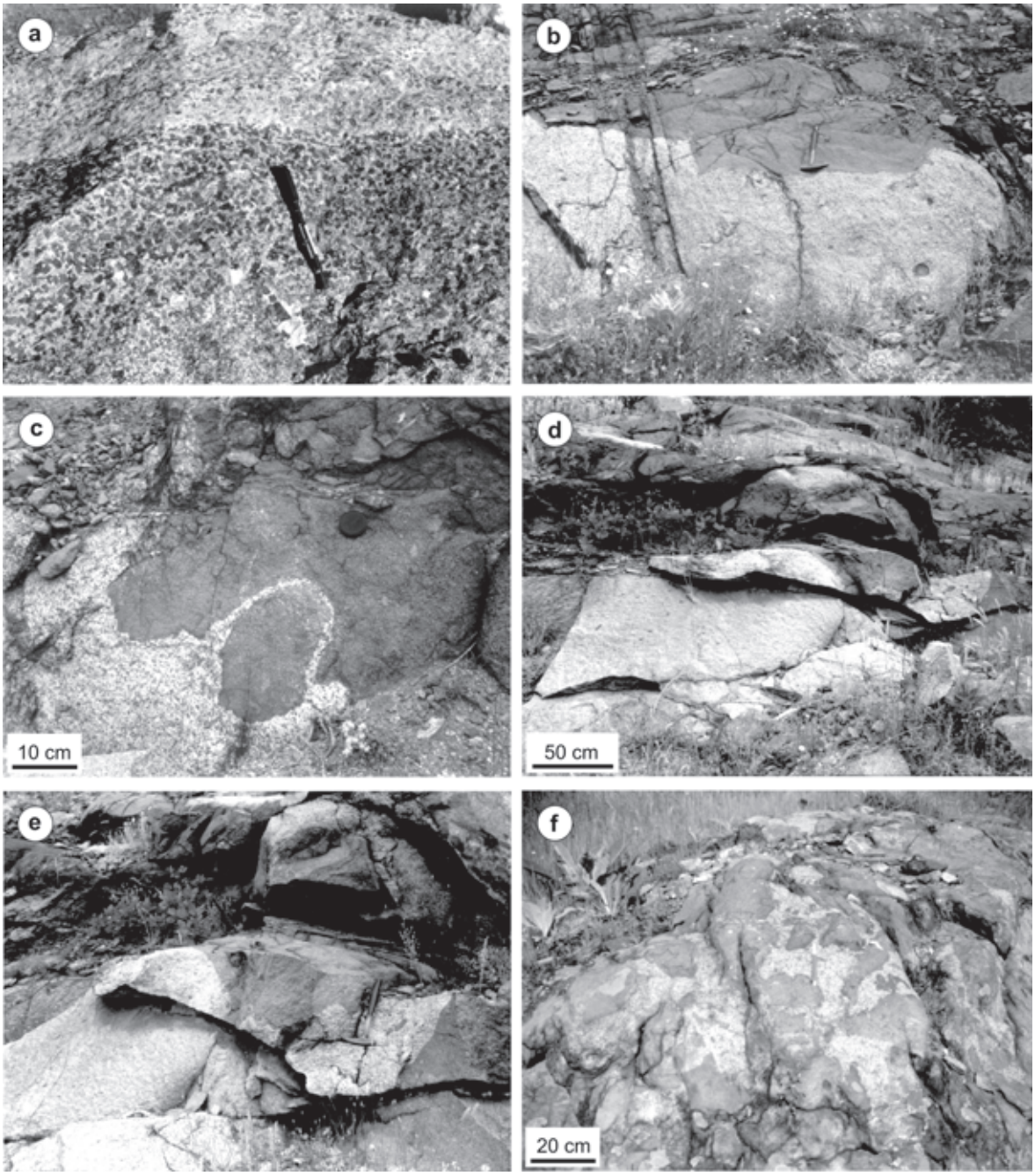

Fig. 8. Structural peculiarities of the gabbro sheets and contact zone between gabbro and granodiorite. **a** — Coarse-grained gabbros and/or gabbro-diorites represent the inner parts of the sheets. **b** — Chilled zone in the periphery of gabbro sheet along the contact with granodiorite. **c** and **d** — "load-cast" and **e** — "flame" structures along the basis of mafic sheet. **f** — Mafic microgranular enclaves often dominate over the host granitoid matrix.

local stresses due to stopping and lower pressure conditions during magma emplacement.

The girdle scattering of Kmin observed at more than 1/3 of the studied sites is not related to uncertainty of measurement, allowing the determination of significant magnetic zone axis. In almost all of these sites, the latter coincides well with the magnetic lineation, which thus could be of intersection or stretching type. The coincidence between visible magmatic and magnetic lineations indicates that the orientation of magnetic lineation is not related to superimposed magnetic fabrics. The coincidence of the magnetic zone axis and visible lineation is therefore related to conditions of magma emplacement.

Corrected anisotropy degree

The corrected degree of anisotropy P' (Jelinek 1981), indicating the "intensity" of the fabric, ranges from 1.02 to 1.54.

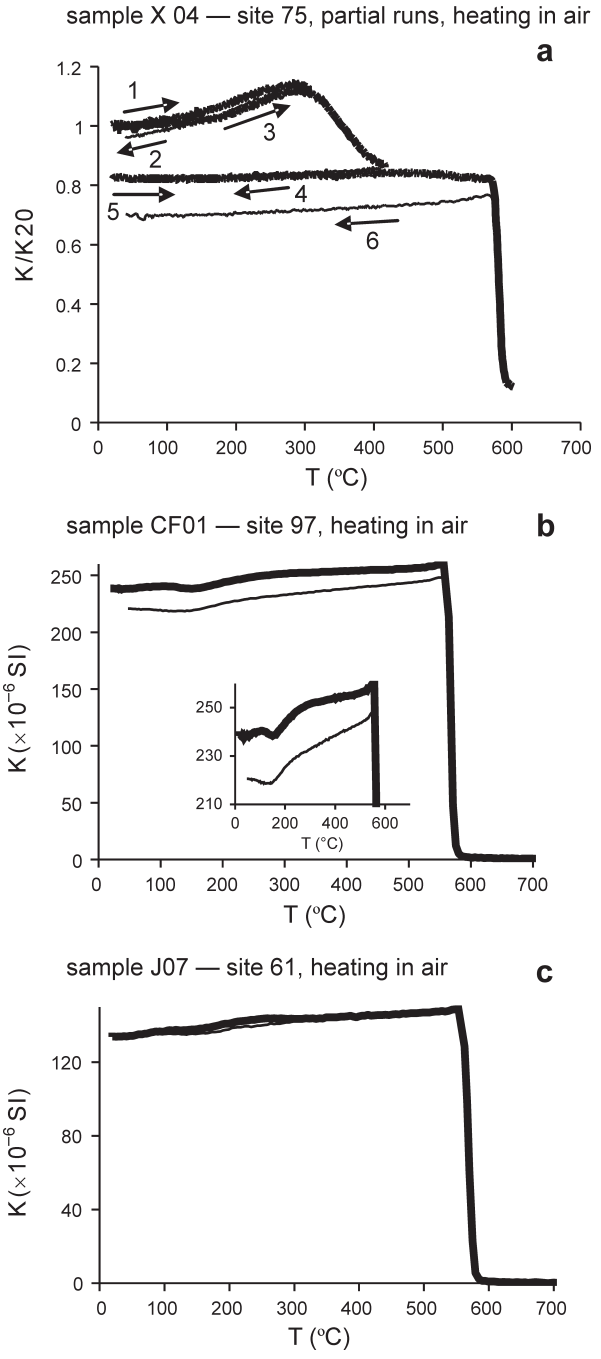

Fig. 9. a — High-temperature behaviour of magnetic susceptibility for site 75 with partial susceptibility runs (subsequent cycles indicated by numbers) for revealing chemical changes during heating. **b** — Thermomagnetic K(°T) analysis for sample from site 97. The inset shows on an enlarged scale the upper part of the curves for revealing peculiarities in the moderate temperature range (120–200 °C). **c** — Thermomagnetic analysis for sample from site 61. The heating and cooling curves coincide. Heating curves are presented by thick line, cooling — by thin lines.

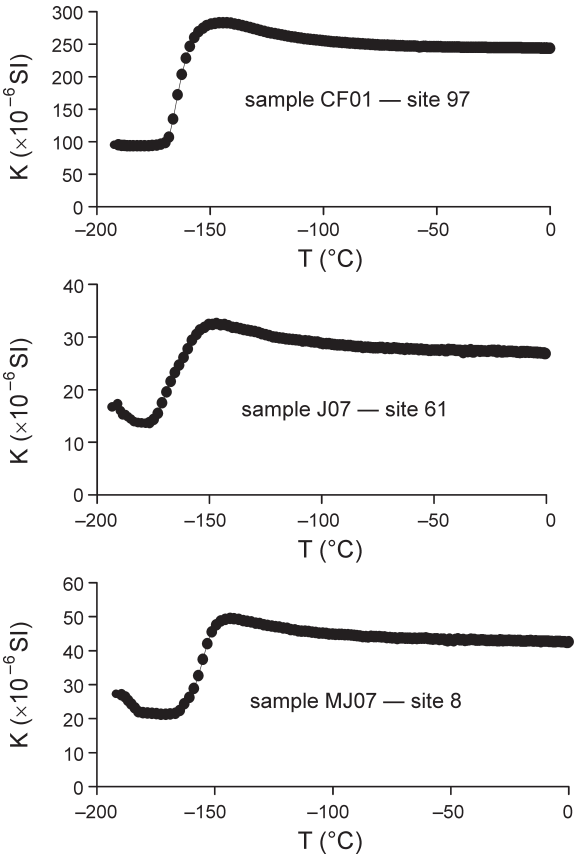

Fig. 10. Low-temperature behaviour of magnetic susceptibility for selected samples.

A dependence of P' on the mean susceptibility K (Fig. 13) suggests some partial mineralogical control on P' values (Henry 1980), namely an increased content of magnetite, which should be more anisotropic than the low susceptibility components. The obtained low P' values and their relatively good clustering around mean values of 1.06–1.08 for Elshitsa and Lesichovo granites and granodiorites define the existence of low strain in these levels. On the contrary the other intrusions are characterized by wider P' distribution, reflecting the proximity of the sampled sites to the main shear zone. This underlines the major importance of the IYSZ for the development of the magnetic fabric. The high P' values observed in the middle part of the Plana basites and gabbro-diorites together with the orientation of the magnetic lineation suggests the presence of high strain level possibly due to an unrevealed shear zone. The lateral pattern of P' distribution (Fig. 14) and the observed systematically higher P' values for sites close to the IYSZ and in the western part (Fig. 15) unambiguously show the major role of the tectonic strain on the magnetic fabric. The magnetic fabric, being related to magmatic stage, shows that magma was emplaced when the shear zone was the area with the maximum strain, magma flow being driven by the tectonic conditions.

Shape factor T

The shape of the magnetic susceptibility ellipsoid deduced from the T parameter (Jelinek 1981) may give information about the deformation pathway in different geological formations where progressive tectonic development occurred

Table 2: Hysteresis parameters and ratios for selected samples. **Hc** — coercive force; **Hcr** — coercivity of remanence; **Js** — saturation magnetization; **Jrs** — saturation remanence; **Xpara** — "paramagnetic" susceptibility calculated from the linear high-field part of the hysteresis loops.

Site	Sample	Hc (mT)	Hcr (mT)	Js (mAm^2/kg)	Jrs (mAm^2/kg)	Hcr/Hc	Jrs/Js	Xpara ($x10^{-9}m^3/kg$)
Elshitsa granodiorites								
90	bl01	12.2	50.5	520	47	4.14	0.09	95
84	bg07	3.8	41	121	3.67	10.8	0.03	43.2
20- vein	mv01	11.3	42.5	447	36.7	3.76	0.08	58.9
24-vein	mdd05	1.51	20.3	226	2.26	13.5	0.01	59.7
75-xenol.l.	x04	4.03	47.2	455	14	11.7	0.03	88.3
Lesichovo leucocratic granites								
42	mww03	para						
89	bk03	para						
40	mvv05	9.92	66.9	536	41.1	6.75	0.08	75.1
Varshilo granites								
92	ca06	1.39	22	411	4.12	15.9	0.01	66.1
94	cc04	1.11	15.7	229	2.54	14.1	0.01	51.3
17	ms06	2.12	27.8	777	10.9	13.1	0.01	51.4
47	a03	1.28	16.2	1423	15.3	12.7	0.01	177
47B	c03	22.9	56.3	61.7	13.8	2.46	0.22	39.8
36-xenol.l.	mqq04	4.1	26.4	1264	39.3	6.48	0.03	104
Gutsal granodiorites								
99	ch03	2.1	22.9	1412	20.5	10.9	0.01	88.8
97	cf01	3.47	24	1785	56.5	6.92	0.03	132
27	mgg01	3.01	25.4	1199	31.6	8.46	0.03	74
30	mjj03	2.76	23.4	932	19.9	8.48	0.02	88.5
57	f05	10.9	56.8	403	31.5	5.24	0.08	55.5
98	cg09	1.45	22.3	658	7.3	15.4	0.01	53.2
71	u07	9.98	44.3	599	47.3	4.44	0.08	310
61	j07	5.42	34.8	736	25.5	6.42	0.03	78.3
59-vein	h02	8.54	50.8	73.7	4.15	5.95	0.06	14.6
Plana basites, gabrodiorites–monzo gabro								
63	l09	1.59	22.6	352	4.85	14.21	0.014	183
65	n06	0.66	6.54	1128	6.84	9.96	0.01	191
66	k06	3.44	27.7	653	17.5	8.06	0.03	46
69	r02	0.9	14.3	1355	11.1	15.8	0.01	186
68	q04	1.71	17.3	943	15.5	10.1	0.02	170

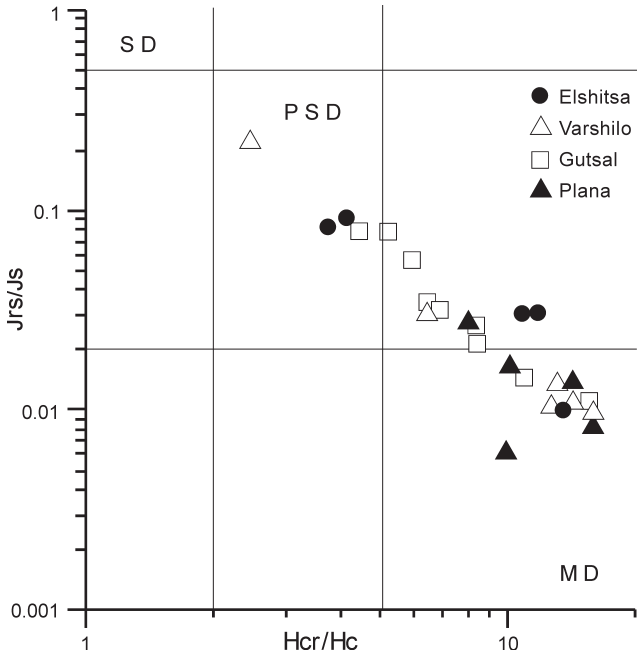

Fig. 11. Day diagram (Day et al. 1977) for samples subjected to hysteresis measurements.

(Borradaile 1988; Borradaile & Henry 1997). As far as P' lateral distribution (Fig. 14) underlines the role of the IYSZ for the development of the magnetic fabric, the P'-T diagram of Jelinek (1981) was plotted separating the samples according to the field observations (no visible data, magmatic HT or M-LT foliation and lineation). From Figs. 13 and 14, it is obvious that the sites, possessing low anisotropy P' and more scattered principal axes, generally situated away from the shear zone, are characterized by variable shape of the susceptibility ellipsoid, ranging from rod-shaped (T=–1) through neutral to oblate (T=+1). On the other hand, sampling sites, for which magmatic and/or HT structures are visible, show a tendency to be closer to the neutral form with increasing degrees of anisotropy (Fig. 13). This dominant behaviour may be related to the shape of a strain ellipsoid corresponding to flow conditions related to a simple shear or transpressive tectonic regional regime.

Lateral variations of the shape parameter T (Fig. 16) show that the oblate fabric is largely dominant, except close to the shear zones. This increased stretching close to the shear zones points out the role of shearing during magma emplacement. In several locations where magnetite content is relatively low, the mineralogical source of prolate magnetic susceptibility ellipsoids could be the presence of linear orientation of the hornblende grains.

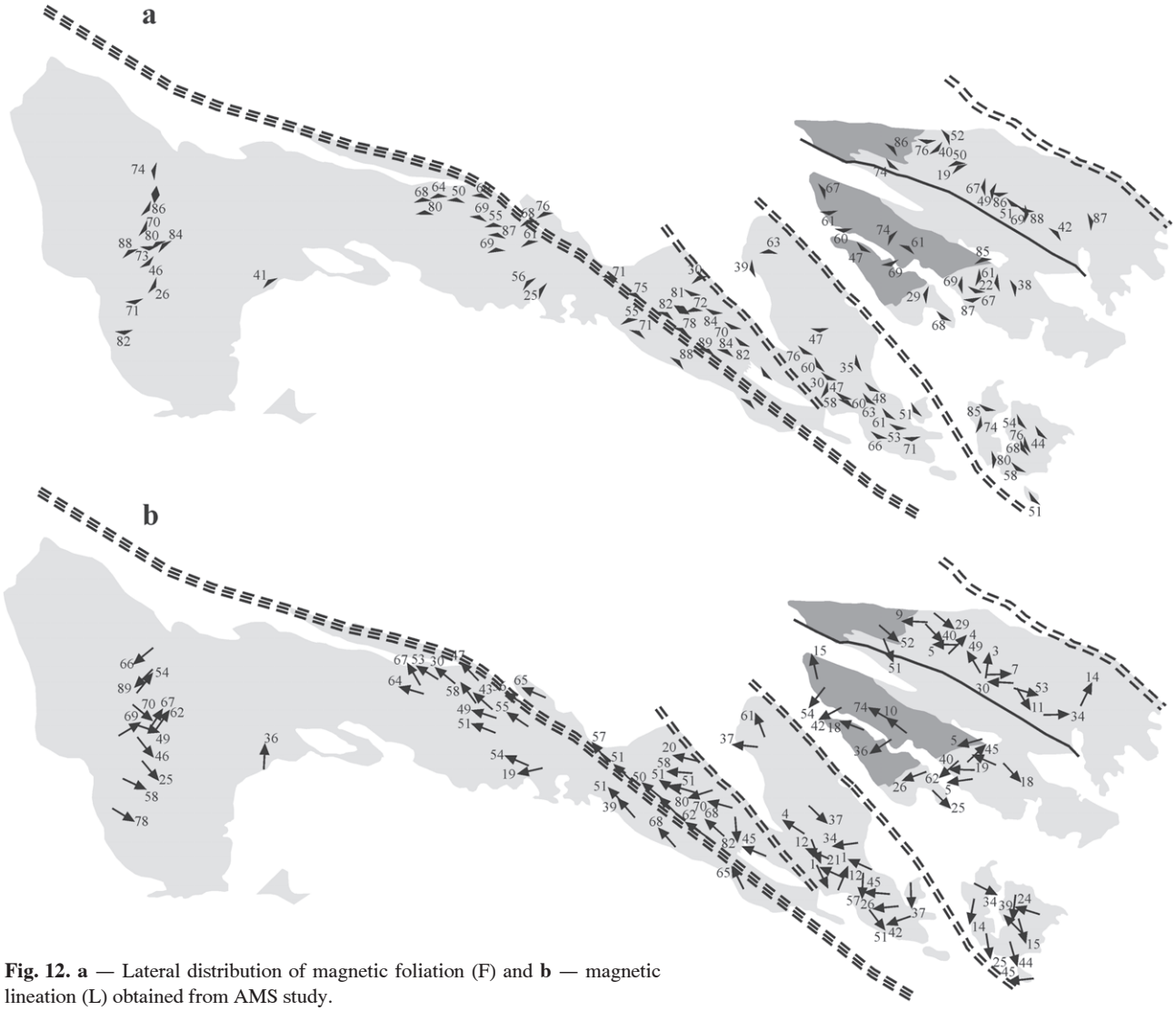

Fig. 12. a — Lateral distribution of magnetic foliation (F) and **b** — magnetic lineation (L) obtained from AMS study.

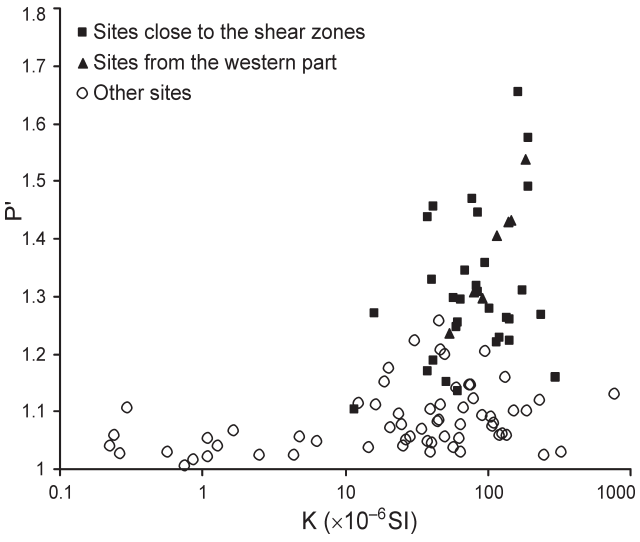

Fig. 13. K-P' dependence for sites close to the shear zone, western part and away from IYSZ.

Comparison of magnetic fabric of granitoids and gabbro bodies

Most of the plutons studied have the characteristics of well-layered intrusions: their lower parts consist of crystal-rich granodiorites and granites and the upper parts of granites poor in felsic crystals. Between the two parts, comparatively large sheet-like bodies of gabbro and gabbrodiorites are placed below swarms of basic enclaves. The observed magnetic fabric in both granitic and basic facies almost always coincide in a number of outcrops (Fig. 12). The basic magma, coming from deeper crust levels therefore permeated along the shear zone in the same dynamic conditions. Thus, both petrostructural and AMS data give good ground to consider the magmatic complex resulting from mingling of two different magma melts — granitic and basic.

Magnetic fabric of dykes

Dyke planes in the studied plutons are often parallel to magmatic and later foliations (Figs. 1, 2d). The field orienta-

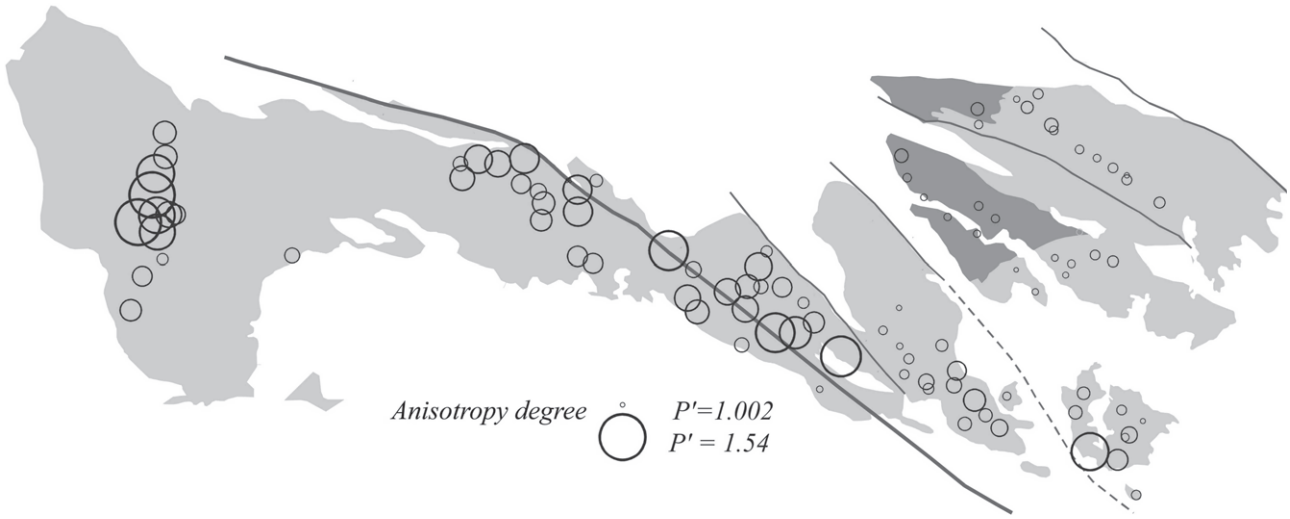

Fig. 14. Lateral distribution of the corrected degree of anisotropy P'.

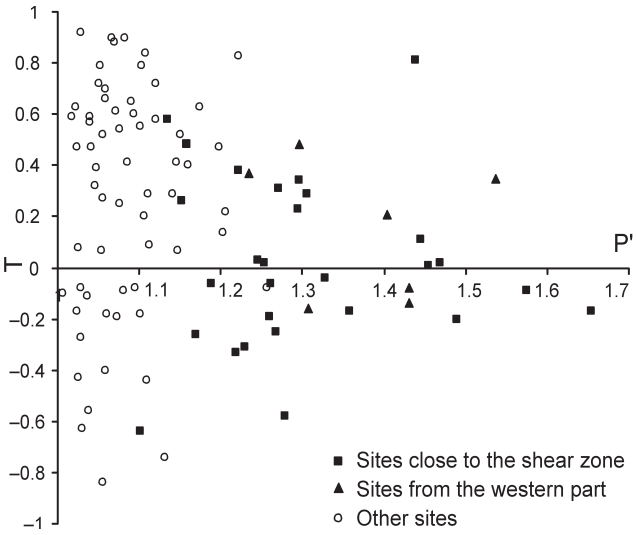

Fig. 15. Plot of shape parameter T versus corrected degree of anisotropy P' for sites, situated at different distance from the main shear zone.

tion of dykes has in fact, except for site 61A, typical Sredna Gora direction (130–150° trends) with relatively high dip of 50–90°. In these cases (except site 23B), the magnetic foliation is parallel to the dyke walls (Fig. 17), but it also agrees with the magnetic foliation in the host granitoids. In site 23B, the shift between dyke wall orientation and magnetic foliation is about 40°. Such a shift is often explained by an imbrication phenomenon (Knight & Walker 1988) caused by the flow gradient of magma along the walls. In this case, symmetrical deviation of the different axes is observed along the two walls relative to the central part of the dyke. That is not the case here, the fabric being similar in the whole dyke. In addition, no imbrication has been observed in our case close to the walls of all the studied dykes. It is therefore probably related to strain effect after filling of the dyke (Henry 1974a,b). In site 23B, magnetic foliation in the host granitoids moreover has a slightly different orientation relative to the other sites, and its orientation coincides with that obtained within the dyke. This similar orientation of the magnetic foliation confirms the major role of the strain effect for the origin of the magnetic fabric within the dyke. The same interpretation is proposed for the dyke of site 61A, which plunges to the South and has an orientation, different from typical the Sredna Gora direction. The orientation of the magnetic foliation within this dyke again is different from that of the dyke plane, but similar to that of the magnetic foliation, locally different from the main part of the plutons, in the host granitoids. Dykes were therefore emplaced as late intrusions within granitic bodies already solidified but they underwent almost similar strain to the granite when the latter was still in the magmatic state.

However, Kmax within a dyke mostly has a higher inclination than within the granitoids. This could indicate a slightly different strain context. In addition, the degree of magnetic anisotropy varies from 1.01 up to 2.02 and is relatively high in comparison with that obtained in the host granitoids.

Discussion

Our interpretation is based on the structural field and AMS evidence for the controlling role of the IYSZ and related shear zones as well as field evidence for magma mingling processes.

The field and laboratory structural investigations point to dextral oblique-slip kinematics of the shear zones. Macro- and micro-scale kinematic criteria within the deformed igneous and metamorphic host rocks show stable dextral oblique shearing in the high-temperature and moderate to low-temperature domains (Figs. 5, 6 and 7).

In the field, magmatic planar and linear structures and superimposed high- to moderate- and low-temperature foliation and lineation generally show the same orientations.

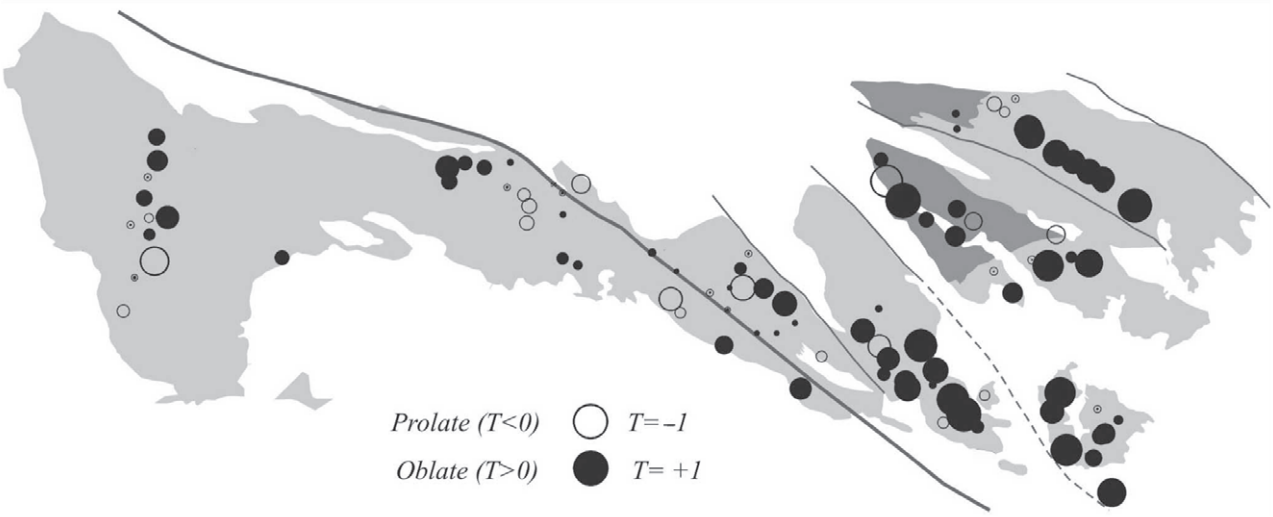

Fig. 16. Lateral variation of shape parameter T.

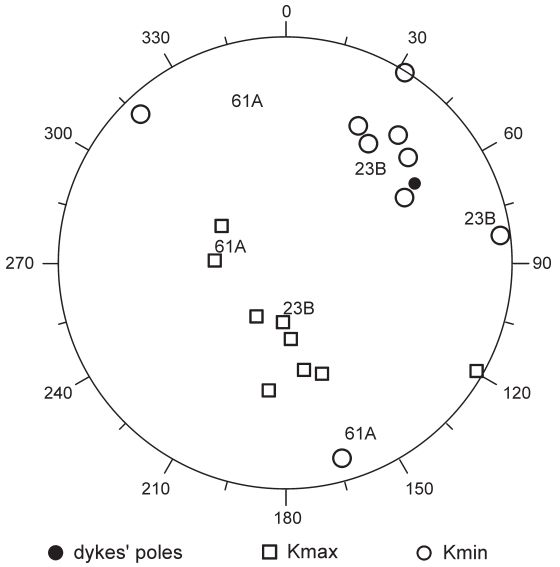

Fig. 17. Stereographic projection on the lower hemisphere of dyke's orientation and the direction of Kmax.

Primary magmatic flow structures near the contacts of the plutons are common. In such places magmatic foliation is parallel to the contact surface and the foliation in the metamorphic host rocks. This conformity can be explained by a syntectonic emplacement (Archanjo et al. 1994; Bouchez 1997; Schofield & D'Lemos 1998). In spite of the apparent isotropic structure of the studied plutons, strips of well pronounced magmatic foliation from the inner parts of the plutons are adjacent and parallel to the mylonites of the IYSZ and its related shear zones. Away from the areas of intensive deformation, the magmatic flow structures are less pronounced and oblique to the strike of the shear zones. A smooth transition from magmatic foliation near the shear zones to high-temperature to moderate- and low-temperature deformational structures within the shear zones argues for a deformation during the time of emplacement (Bouchez et al. 1981, 1992; Gapais 1989; Ghosh 1993; Miller & Paterson 1994; Saint-Blanquat & Tikoff 1997; Zurbriggen et al. 1997).

The field assumption of a transition from magmatic to superimposed deformational structures and syntectonic character of the studied plutons is confirmed by microstructural investigations. Thin sections, displaying magmatic foliation and submagmatic deformation (Fig. 2 and Fig. 4.) as well as structures of high- to low-temperature overprint (Fig. 5 and Fig. 6), all of them with the same kinematics, give evidence of a continuous deformation process. The long-lasting deformational process affected both crystal-melt mush and, subsequently, crystallized igneous rocks. The progressive deformation and exhumation of the system have led to the localization/partitioning of deformation and the formation of narrow ultramylonite bands within the inner parts of the shear zones. Static recrystallization under relatively high temperatures in the high-strain mylonite bands within the IYSZ in the vicinity of the Gutsal pluton (Fig. 5c,e,f) reveals that the last stage of the shear zone activity was followed by heating due to the emplacement of the Gutsal granodiorite at ~75 Ma.

Direct observations of strain in the granitoids were possible only in limited areas, the rocks being mostly apparently isotropic. They were completed by AMS data which point to the presence of magnetic foliation and lineation largely developed in all the intrusive bodies. In fact, in the few AMS sites where visible magmatic structures are present, these structures show good agreement with AMS data, confirming the mainly magmatic origin of the magnetic fabric. These AMS data then confirm at a more regional scale the syntectonic character of the studied plutons and intensive shearing during and after their emplacement.

The foliation and stretching lineation of the metamorphic host rocks are parallel to the shear zone structures or parallel to the strike of plutonic contacts. Such features indicate intensive superimposed shearing of the metamorphic rocks in the studied area during the intrusion of the plutons.

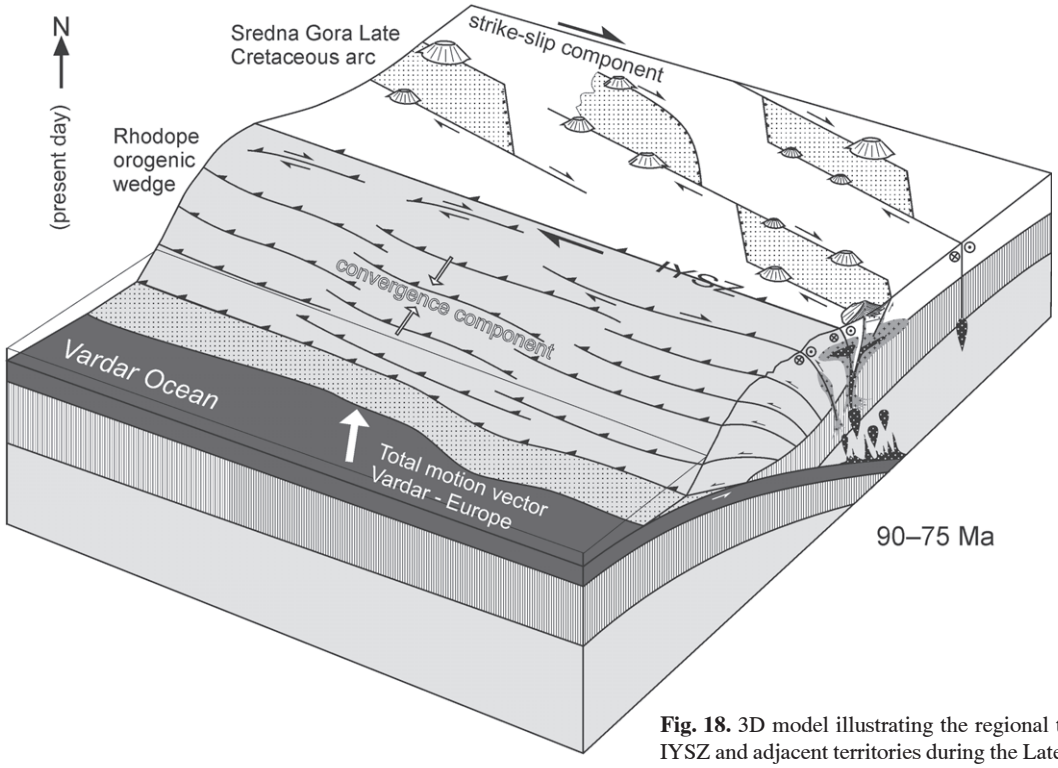

Fig. 18. 3D model illustrating the regional tectonic setting along the IYSZ and adjacent territories during the Late Cretaceous (90–75 Ma).

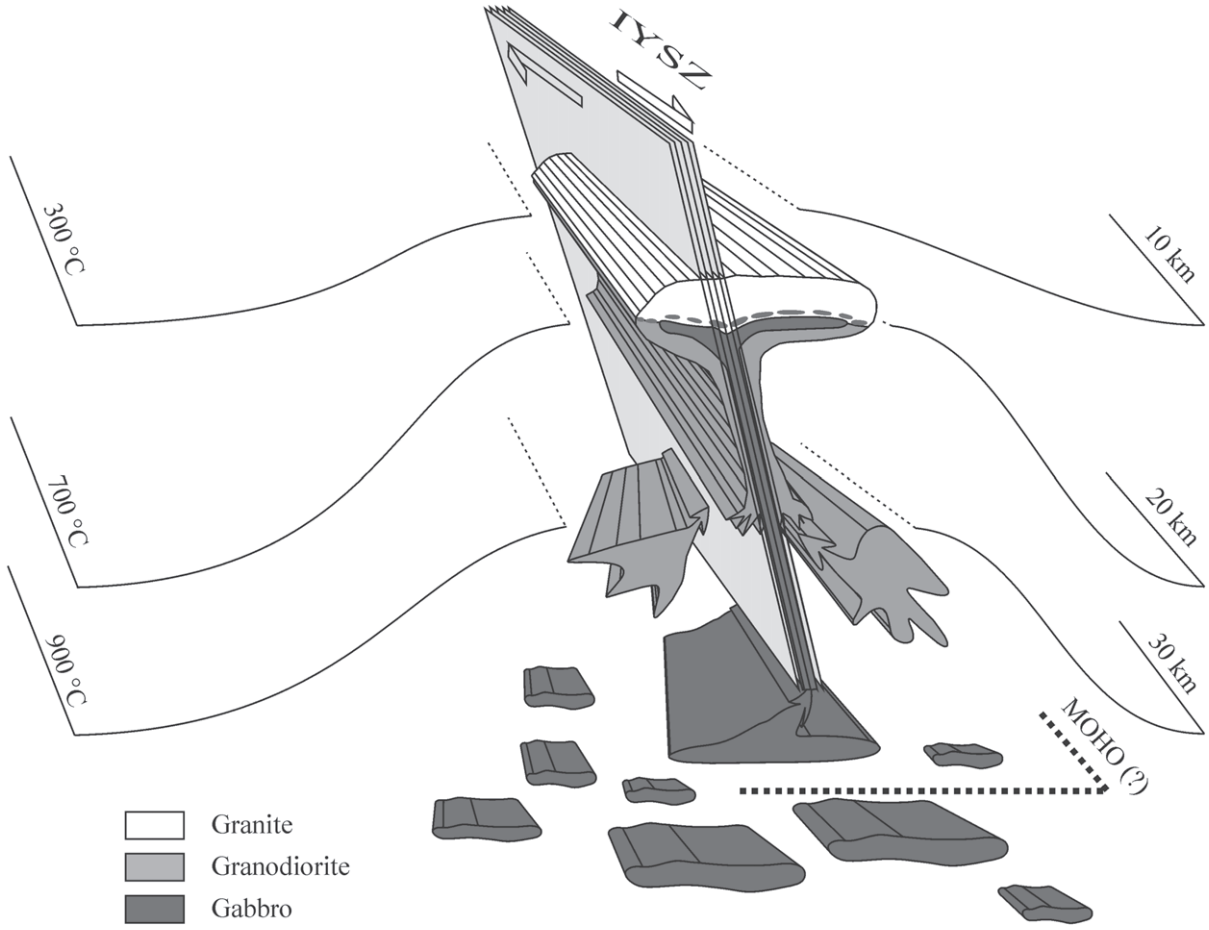

Fig. 19. Hypothetical model of magma drainage along IYSZ (after Ferre et al. 1997, modified).

The mafic varieties and magmatic enclave swarms have a close spatial relationship with the IYSZ and the related shear zones (Fig. 1). This underlines the connection between deformation and magma emplacement. The field relations between mafic and felsic intrusive rocks support an interpretation in terms of magma mingling. Chilled, sharp and relatively linear contacts of the gabbroic sheets with the granodiorite host (Fig. 8b) are evidence of fast cooling during mafic magma crystallization. The mafic melt has intruded into a partly crystallized granitoid magma chamber (see Wiebe & Collins 1998). The presence of specific structures such as load casts and flame structures (Fig. 8) at the lower contact of the mafic sheets gives evidence for a viscous state of both felsic and mafic melt at the time of their interaction. Zircon U-Pb ages of granitoids and gabbros confirm contemporaneous crystallization of mafic and felsic constituents of the plutons (Table 1).

Mafic and felsic dykes that crop out within deformed igneous rocks of the studied plutons are parallel to the foliation. Dykes within isotropic parts of the studied intrusive bodies are usually parallel to the strike of IYSZ and related shear zones. This type of development of the dyke system points to a relatively long lasting regional stress system. The latter is supported by both deformed and undeformed dykes observed within the sheared domains.

The lineation (both measured in the field and from the AMS) near the IYSZ generally plunges towards NW at moderate angles, showing that the dextral shearing had a large vertical component with a relative uplift of the northeastern block. This displacement is unrelated to the exhumation of the Rhodope metamorphic rocks because the exhumation would require the opposite vertical component. The Cretaceous-age shearing along the IYSZ could be related to oblique plate convergence along the Vardar suture zone, which was partitioned into southwest-directed thrusting in the Rhodopes and dextral shearing in the hinterland (Fig. 18), as typically observed in subduction zones with oblique convergence (e.g. Platt 1993). On the block-diagram in Fig. 18 we have sketched the situation during the period ~90–75 Ma. It shows a transpressive regime in the vicinity of IYSZ and compressive tectonics to the south in the Rhodope area. To the north and northeast of IYSZ the transcurrent shearing probably had an extensional component leading to the formation of isolated pull-apart and strike-slip sedimentary basins.

Conclusions

Summarizing all the above presented data, as well as mechanisms known from the literature (Michael 1991; Ferre et al. 1997; Wiebe & Collins 1998; Steenken et al. 2000; Rosenberg 2004), we can propose the following schematic emplacement mode for the investigated magmatic bodies (Fig. 19).

Upper Cretaceous plutons situated in the southwestern parts of the Sredna Gora Zone resulted from simultaneous syntectonic emplacement (86–75 Ma) of two different magma types — felsic and mafic. Mingling of the two magmas took place in the magma chamber at a depth of 10–15 km, corresponding to the boundary between the upper and middle crust, and at temperatures between 770 and 680 °C (Georgiev & Lazarova 2003).

The different Upper Cretaceous plutonic bodies from the southwestern part of the Sredna Gora Zone present similar magmatic and structural evolutions. Field relationships, petrostructural and magnetic (AMS) data in fact show that magma emplacement and deformation processes have been accomplished in a dextral oblique-slip regime. These deformation processes occurred during magmatic and post-magmatic stages and for the latter under high-, moderate-, and low-temperature conditions The Iskar-Yavoritsa shear zone and the related synthetic shear zones played a major role in the evolution of the magmatic system. These zones originated 106–100 Ma ago (Velichkova et al. 2001) and represented a main drainage channel for both granitoid and mafic melts. The deformation along the shear zone ceased with the emplacement of the undeformed ~75 Ma Gutsal pluton, which has intruded as sills into the Iskar-Yavoritsa mylonites.

Acknowledgments: This work was supported by the NATO Collaborative Research Grant No. CRG.LG973943. N.F. was supported by DFG Grant FR 700/10-1 and DAAD Project PPP Bulgaria. We would like to thank F. Hrouda, M. Putiš and I. Petrík for careful and constructive reviews. N.G. also thanks Z. Cherneva, A. Lazarova and I. Gerdjikov for fruitful discussions and to Prof. Ch. Pimpirev and the Bulgarian Antarctic Institute for responsiveness, technical and financial support.

References

Acef K., Liégeois J.P., Ouabadi A. & Latouche L. 2003: The Anfeg post-collisional Pan-African high-K calc-alkaline batholith (Central Hoggar, Algeria), result of the LATEA microcontinent metacratonization. *J. Afric. Earth Sci.* 37, 295–311.

Amov B.G., Arnaudov V.S. & Pavlova M.A. 1982: Lead isotope data and age of granitoid and metamorphic rocks from Sredna Gora and Pirin. *Compt. Rend. Acad. Bulg. Sci.* 35, 11, 1535–1537.

Archanjo C.J., Bouchez J.L., Corsini M. & Vauchez A. 1994: The Pombal granite pluton: magnetic fabric, emplacement and relationships with the Brasiliano strike-slip setting of the NE Brasil. *J. Struct. Geol.* 16, 323–337.

Barbarin B. & Didier J. 1992: Genesis and evolution of mafic microgranular enclaves trough various types of interaction between coexisting felsic and mafic magmas. *Trans. Roy. Soc. Edinburgh, Earth Sci.* 83, 145–153.

Belmustakova H. 1984: Petrographic description of granitoid plutons from Ihtiman Sredna Gora Region. *Geochem. Mineral. and Petrology* 18, 56–83.

Bergougnan H. & Fourquin C. 1980: Un ensemble d'éléments communs à une marge active alpine des Carpathes méridionales à l'Iran central: le domaine iranobalkanique. *Bull. Soc. Géol. France* 12, 61–83.

Berza T., Constantinescu E. & Vlad S.-E. 1998: Upper Cretaceous magmatic series and associated mineralization in the Carpathian-Balkan orogen. *Resource Geology* 48, 4, 291–306.

Bleil U. & Petersen N. 1982: Magnetic properties of minerals. In: Bleil U. & Petersen N. (Eds.): Landolt-Bornstein numerical data and functional relationships in science and technology. Group V: Geophysics and space research. Vol. 1. Physical properties of rocks. Subvol. B. *Springer*, New York, 1–346.

Boccaletti M., Manetti P. & Peccerillo A. 1974: The Balkanids as an instance of back-arc thrusts belt: Possible relation with the Hellenids. *Geol. Soc. Amer. Bull.* 85, 1077–1084.

Boccaletti M., Manetti P., Peccerillo A. & Stanisheva-Vasileva G. 1978: Late Cretaceous high-potassium volcanism in Eastern Srednogorie, Bulgaria. *Geol. Soc. Amer. Bull.* 89, 439–447.

Borradaile G.J. 1988: Magnetic susceptibility, petrofabrics and strain. *Tectonophysics* 156, 1–20.

Borradaile G.J. & Henry B. 1997: Tectonic applications of magnetic susceptibility and its anisotropy. *Earth. Sci. Rev.* 42, 49–93.

Bouchez J.-L. 1997: Granite is never isotropic: an introduction to AMS studies of granitic rocks. In: Bouchez J.-L., Hutton D.H.W. & Stephens W.E. (Eds.): Granite: from segregation of melt to emplacement fabrics. *Kluwer Academic Publishers*, Dordrecht, 95–112.

Bouchez J.-L., Guillet P. & Chevalier F. 1981: Structures d'ecoulement liees a la mise en place du granite de Guerande (Loire-Atlanticue, France). *Bull. Soc. Geol. France* 23, 387–399.

Bouchez J.-L., Delas C., Gleizes G., Nedelec A. & Cuney M. 1992: Submagmatic microfractures in granites. *Geology* 20, 35–38.

Boyadjiev St. 1979: The Srednogorie neointrusive magmatism in Bulgaria. *Geochem. Mineral. and Petrology* 10, 74–90.

Castro A. 1987: On granitoid emplacement and related structures. A review. *Geol. Rdsch.* 76, 101–124.

Carrigan C., Mucasa S., Haydutov I. & Kolcheva K. 2005: Age of Variscan magmatism from the Balkan sector of the orogen, central Bulgaria. *Lithos* 82, 125–147.

Carrigan C., Mucasa S., Haydutov I. & Kolcheva K. 2006: Neoproterozoic magmatism and Carboniferous high-grade metamorphism in the Sredna Gora Zone, Bulgaria: An extension of Gondwana-derived Avalonian-Cadomian belt? *Precambrian Res.* 147, 3–4, 404–416.

Dabovski Chr. 1980: Magmotectonic feature of Upper Cretaceous intrusives in the Srednogorie zone: field and experimental evidence for a rift model. *Geol. Balcanica* 10, 1, 15–29.

Dabovski Chr. 1988: Fissure intrusions in the Srednogorie — structural analysis, mathematical and laboratorial models. *BAS,* Sofia, 1–184 (in Bulgarian, abstract in English).

Day R., Fuller M. & Schmidt V.A. 1977: Hysteresis properties of titanomagnetites: grain size and compositional dependence. *Phys. Earth. Planet. Int.* 13, 260–267.

Dekkers M.J. 1990: Magnetic monitoring of pyrrhotite alteration during thermal demagnetization. *Geophys. Res. Lett.* 17, 779–782.

Dimitrov Str. 1933: Geologische und petrographische Untersuchungen an den sudostlichen Abhangen der Witoscha und an den nordlichen Teilen der Plana Planina (S.W. Bulgarien), mit besonderer Berucksichtigung der Kontakthofe der Intrusivgesteine. *Ann. Univ. Sofia, Fac. Phys.-Math.* 30, 3, 41–130.

Dunlop D. 2002: Theory and application of the Day plot (Mrs/Ms versus Hcr/Hc). 1. Theoretical curves and test using titanomagnetite data. *J. Geophys. Res.* 107, EPM 4, doi, 10.1029/ 2001JB000486.

Dunlop D. & Özdemir Ö. 1997: Rock magnetism: Fundamentals and frontiers. *Cambridge University Press*, 1–573.

Ferre E., Gleizes G., Djouadi M.T., Bouchez J.-L. & Ugodulunwa F.X.O. 1997: Drainage and emplacement of magmas along an inclined transcurrent shear zone: petrophysical evidence from granite-charnockite poluton (Rrahama, Nigeria). In: Bouchez J.-L., Hutton D.H.W. & Stephens W.E. (Eds.): Granite from segregation of melt to emplacement fabrics. *Kluwer Academic Publishers*, Dordrecht, 253–274.

Gapais D. 1989: Shear structures within deformed granites: Mechanical and thermal indicators. *Geology* 17, 1144–1147.

Georgiev N. & Lazarova A. 2003: Magma mixing in Upper Cretaceous plutonic bodies in the Southwestern parts of the Central Sredna gora zone, Bulgaria. *Compt. Rend. Bulg. Acad. Sci.* 56, 4, 47–52.

Ghosh S.K. 1993: Structural geology. *Pergamon Press*, Oxford, 1–589.

Henry B. 1974a: Sur l'anisotropie de susceptibilité magnétique du granite récent de Novate (Italie du nord). *Compt. Rend. Acad. Sci. Paris* 278C, 1171–1174.

Henry B. 1974b: Microtectonique et anisotropie de susceptibilité magnétique des filons aplitiques et pegmatitiques récents du massif du Bergell (frontière italo-suisse). *Compt. Rend. Acad. Sci. Paris* 279C, 385–388.

Henry B. 1980: Contribution à l'étude des propriétés magnétiques de roches magmatiques des Alpes: Conséquences structurales, régionales et générales. *Trav. Lab. Tectonophysique Paris,* CRE 80/07, 1–528.

Henry B. 1997: The magnetic zone axis: a new element of magnetic fabric for the interpretation of magnetic lineation. *Tectonophysics* 271, 325–331.

Henry B. & Le Goff M. 1995: Application de l'extension bivariate de la statistique de Fisher aux données d'anisotropie de susceptibilité magnétique: intégration des incertitudes de mesure sur l'orientation des directions principales. *Comt. Rend. Acad. Sci. Paris* 320, II, 1037–1042.

Henry B., Bayou B., Derder M.E.M., Djellit H., Ouabadi A., Merahi M., Baziz K., Khaldi A. & Hemmi A. 2004: Emplacement and fabric-forming conditions of the Alous-En-Tides granite, eastern border of the Tin Seririne/Tin Mersoï basin (Algeria): magnetic and visible fabrics analysis. *J. Struct. Geol.* 26, 1647–1657.

Hext G. 1963: The estimation of second-order tensors, with related tests and designs. *Biometrika* 50, 353.

Hippertt J.F.M. 1993: "V"-pull-apart microstructures: a new shear-sense indicator. *J. Struct. Geol.* 15, 12, 1393–1403.

Hrouda F., Chlupachova M. & Rejl L. 1971: The mimetic fabric of magnetite in some foliated granodiorites, as indicated by magnetic anisotropy. *Earth Planet. Sci. Lett.* 11, 381–384.

Hsu K.J., Nachev I.K. & Vuchev V.T. 1977: Geologic evolution of Bulgaria in light of plate tectonics. *Tectonophysics* 40, 245–256.

Hutton D.H.W. 1988: Granite emplacement mechanisms and tectonic controls: Infeences from deformation studies. *Roy. Soc. Edinburgh Trans., Earth Sci.* 79, 245–255.

Hutton D.H.W. 1997: Granite is never isotropic: Syntectonic granites and the principle of effective stress: a general solution to the space problem. In: Bouchez J.-L., Hutton D.H.W. & Stephens W.E. (Eds.): Granite: from segregation of melt to emplacement fabrics. *Kluwer Academic Publishers*, Dordrecht, 189–197.

Ivanov Z. 1988: Aperçu général sur l'évolution géologique et structurale du massif des Rhodopes dans le cadre des Balkanides. *Bull. Soc. Geol. France* 8, IV, 2, 227–240.

Ivanov Z. 1989: Structure and tectonic evolution of the central parts of the Rhodope massif. In: Ivanov Z. (Ed.): Guide to excursion e-3. *CBGA 14th Congr. Sofia, Bulgaria*, 56–96.

Ivanov Z., Dimov D., Dobrev S., Kolkovski B. & Sarov S. 2000: Structure, Alpine evolution and mineralizations of the Central Rhodopes area (South Bulgaria). In: Ivanov Z. (Ed.): Guide to excursion B, ABCD-GEODE 2000 Workshop, Borovets, Bulgaria, 1–50.

Jankovic S. 1977: Major Alpine ore deposits and metallogenic units in the northeastern Mediterranean and concepts of plate tectonics. In: Metallogeny and plate tectonics in the northeastern Mediterranean. *Fac. Min. Geol. Belgrad Univ. Edit.*, 105–171.

Jankovic S. 1997: The Carpatho-Balkanides and adjacent area: a sector of the Tethyan Eurasian metallogenic belt. *Mineralium Deposita* 32, 426–433.

Jelinek V. 1978: Statistical processing of magnetic susceptibility measured in groups of specimens. *Stud. Geophys. Geod.* 22, 50–62.

Jelinek V. 1981: Characterization of magnetic fabric of rocks. *Tectonophysics* 79, 563–567.

Knight M.D. & Walker G.P.L. 1988: Magma flow directions in

dikes of the Koolau complex, Oahu, dterminated from magnetic fabric studies. *J. Geophys. Res.* 93, 4301–4319.

Kruhl J.H. 1996: Prism- and basal-plane parallel subgrain boundaries in quartz: a microstructural geothermobarometer. *J. Metamorph. Geology* 14, 581–589.

Michael P. 1991: Intrusion of basaltic magma into a crystallizing granitic magma chamber: The Cordillera del Paine pluton in southern Chile. *Contr. Mineral. Petrology* 108, 396–418.

Miller R.B. & Paterson S.R. 1994: The transition from magmatic to high-temperature solid-state deformation: implications from the Mount Stuart batholith, Washington. *J. Struct. Geol.* 16, 853–865.

Mitchell A.H.G. 1996: Distribution and genesis of some epizonal Zn-Pb and Au provinces in the Carpathian–Balkan region. *Trans. Inst. Mining and Metallurgy* (*Section B: Applied Earth Sci.*) 105, 127–138.

Nachev I.K. 1978: On the Upper Cretaceous basin model in the Srednogorie zone. *Compt. Rend. Bulg. Acad. Sci.* 31, 2, 213–216.

Neubauer F. 2002: Contrasting Late Cretaceous with Neogene ore provinces in the Alpine-Balkan-Carpathian-Dinaride collision belt. In: Blundell D.J., Neubauer F. & von Quadt A. (Eds.): The major ore deposits in an evolving orogen. *Geol. Soc. London, Spec. Publ.* 204, 81–102.

Passchier C.W. & Trouw R.A.J. 2005: Microtectonics. 2nd, revised and Enlarged Edition. *Springer–Verlag*, 1–366.

Paterson S.R. & Fowler T.K. 1993: Re-examining pluton emplacement processes. *J. Struct. Geol.* 15, 191–206.

Peytcheva I. & von Quadt A. 2003: U-Pb-zircon isotope system in mingled and mixed magmas. An example from Central Srednogorie, Bulgaria. *Geophys. Res. Abstr.* 5, 09177.

Peytcheva I., Von Quadt A., Kamenov B., Ivanov Zh. & Georgiev N. 2001: New isotope data for Upper Cretaceous magma emplacement in the Southern and South-Western Parts of Central Srednogorie. *Rom. J. Miner. Depos. ABCD-GEODE 2001 Romania Abstr. Vol.,* 82–83.

Platt J.P. 1993: Mechanics of oblique convergence. *J. Geophys. Res.* 98, 16239–16256.

Roman-Berdiel T., Gapais D. & Brun J.-P. 1997: Granite intrusion along strike-slip zones in experiment and nature. *Amer. J. Sci.* 297, 651–678.

Rosenberg C.L. 2004: Shear zones and magma ascent: A model based on a review of the Tertiary magmatism in the Alps. *Tectonics* 23, TC3002, doi:10.1029/2003TC001526.

Saint-Blanquat M. & Tikoff B. 1997: Granite is never isotropic: development of magmatic to solid-state fabrics during syntectonic emplacement of the Mono Creek granite, Sierra Nevada Batholith. In: Bouchez J.-L., Hutton D.H.W. & Stephens W.E. (Eds.): Granite: from segregation of melt to emplacement fabrics. *Kluwer Academic Publishers*, Dordrecht, 231–252.

Sandulescu M. 1984: Geotectonica Rumaniei. *Editura Tehnica*, Bucuresti, 1–336.

Schofield D.I. & D'Lemos R.S. 1998: Relationships between syntectonic granite fabrics and regional PTtd paths: an example from the Gander-Avalon boundary of NE Newfoundland. *J. Struct. Geol.* 20, 4, 459–471.

Stampfli C.M. & Mosar J. 1999: The making and becoming of Apulia. *Mem. Sci. Geol., Univ. Padua* 51, 141–154.

Steenken A., Siegesmund S. & Heinrichs T. 2000: The emplacement of the Reiserferner Pluton (Eastern Alps, Tyrol): constraints from field observations, magnetic fabrics and microstructures. *J. Struct. Geol.* 22, 1855–1873.

Stipp M., Stünitz H., Heilbronner R. & Schmid S. 2002: The eastern Tonale fault zone: a 'natural laboratory' for crystal plastic deformation of quartz over a temperature range from 250 to 700 °C. *J. Struct. Geol.* 24, 1861–1884.

Tarling D.H. & Hrouda F. 1993: The magnetic anisotropy of rocks. *Chapman and Hall*, London, 1–217.

Tikoff B. & Teyssier C. 1992: Crustal-scale, en-echelon "P-shear" tensional bridges: a possible solution to the batholith room problem. *Geology* 20, 927–930.

Velichkova S., Handler R., Neubauer F. & Ivanov Z. 2001: Preliminary $^{40}Ar/^{39}Ar$ mineral ages from the Central Srednogorie Zone, Bulgaria: Implications for Cretaceous geodynamics. *ABCD-GEODE 2001 Romania, Abstr Vol., Rom. Miner. Depos.,* 112–113.

Velichkova S., Handler R., Neubauer F. & Ivanov Z. 2004: Variscan to Alpine tectonothermal evolution of the Central Srednogorie unit, Bulgaria: constraints from $^{40}Ar/^{39}Ar$ analysis. *Schweiz. Mineral. Petrogr. Mitt.* 84, 133–151.

von Quadt A., Moritz R., Peytcheva I. & Heinrich C. 2005: Geochronology and geodynamics of Late Cretaceous magmatism and Cu-Au mineralization in the Panagyurishte region of the Apuseni-Banat-Timok-Srednogorie belt (Bulgaria). *Ore Geol. Rev.* 27, 95–126.

von Quadt A., Sarov S., Peytheva I., Voinova E., Petrov N., Nedkova K. & Naidenov K. 2006: Metamorphic rocks from northern parts of Central Rhodopes — conventional and in situ U-Pb zircon dating, isotope tracing and correlations. *National Conference "Geosciences 2006", Abstr. Vol.,* 225–228.

Wiebe R.A. & Collins W.J. 1998: Depositional features and stratigraphic sections in granitic plutons: implications for the emplacement and crystallization of granitic magma. *J. Struct. Geol.* 20, 9/10, 1273–1289.

Zurbriggen R., Kamber B., Handy M. & Negler T. 1997: Dating synmagmatic folds: a case study of Schlingen structures in the Strona-Ceneri zone (Southern Alps, northern Italy). *J. Metamorph. Petrology* 17, 403–415.